

# A POROSITY-LENGTH FORMALISM FOR PHOTON-TIRING-LIMITED MASS LOSS FROM STARS ABOVE THE EDDINGTON LIMIT

STANLEY P. OWOCKI

Bartol Research Institute, University of Delaware, Newark, DE 19716

KENNETH G. GAYLEY

Department of Physics and Astronomy, University of Iowa, Iowa City, IA 52242

NIR J. SHAVIV

Racah Institute of Physics, Hebrew University, Giv'at Ram, Jerusalem 91904 Israel

*submitted: 10 May 2004; revised 12 Jul 2004*

## ABSTRACT

We examine radiatively driven mass loss from stars near and above the Eddington limit. Building upon the standard CAK theory of driving by scattering in an ensemble of lines with a power-law distribution of opacity, we first show that the formal divergence of such line-driven mass loss as a star approaches the Eddington limit is actually limited by the “photon tiring” associated with the work needed to lift material out of the star’s gravitational potential. We also examine such tiring in simple continuum-driven models in which a specified outward increase in opacity causes a net outward acceleration above the radius where the generalized Eddington parameter exceeds unity. When the density at this radius implies a mass loss too close to the tiring limit, the overall result is flow stagnation at a finite radius. Since escape of a net steady wind is precluded, such circumstances are expected to lead to extensive variability and spatial structure. After briefly reviewing convective and other instabilities that also can be expected to lead to extensive structure in the envelope and atmosphere of a star near or above the Eddington limit, we investigate how the *porosity* of such a structured medium can reduce the effective coupling between the matter and radiation. Introducing a new “*porosity-length*” formalism, we derive a simple scaling for the reduced effective opacity, and use this to derive an associated scaling for the porosity-moderated, continuum-driven mass loss rate from stars that formally exceed the Eddington limit. For a simple super-Eddington model with a single porosity length that is assumed to be on the order of the gravitational scale height, the overall mass loss is similar to that derived in previous porosity models, given roughly by  $L_*/a_*c$  (where  $L_*$  is the stellar luminosity, and  $c$  and  $a_*$  are the speed of light and atmospheric sound speed). This is much higher than is typical of line-driven winds, but is still only a few percent of the tiring limit. To obtain still stronger mass loss that approaches observationally inferred values near this limit, we draw upon an analogy with the power-law distribution of line-opacity in the standard CAK model of line-driven winds, and thereby introduce a *power-law-porosity* model in which the associated structure has a broad range of scales. We show that, for power indices  $\alpha_p < 1$ , the mass loss rate can be enhanced over the single-scale model by a factor that increases with the Eddington parameter as  $\Gamma^{-1+1/\alpha_p}$ . For lower  $\alpha_p$  ( $\approx 0.5 - 0.6$ ) and/or moderately large  $\Gamma$  ( $> 3 - 4$ ), such models lead to mass loss rates that approach the photon tiring limit. Together with the ability to drive quite fast outflow speeds (of order the surface escape speed), the derived, near-tiring-limited mass loss offer a potential dynamical basis to explain the observationally inferred large mass loss and flow speeds of giant outbursts in  $\eta$  Carinae and other Luminous Blue Variable stars.

*Subject headings:* Stars: winds — Stars: early-type — Stars: mass loss

## 1. INTRODUCTION

Massive, hot, luminous stars – those of spectral types O, B, and WR – continuously lose mass in strong, radiatively driven stellar winds. For these relatively quiescent phases of mass loss (i.e., with mass loss rates ranging up to  $10^{-5} M_\odot/\text{yr}$ ), the central mechanism for coupling the radiation to the outflowing gas is understood to be via *line* opacity, augmented through the systematic Doppler shift of the line-scattering by the velocity gradient associated with the flow acceleration. The inherently non-linear feedback between the line driving and flow acceleration can be solved self-consistently via a formalism first developed by Castor, Abbott, & Klein (1975, here-

after CAK), with modern extensions providing wind solutions that are in remarkably good, quantitative agreement with observational inferences of key wind properties like the mass loss rate and wind flow speed, and with the scaling of these with stellar parameters like the luminosity and gravity.

However, at least some massive stars – observationally identified as the so-called Luminous Blue Variables (LBV’s) – appear to undergo one or more phases of much stronger mass loss. Perhaps the most extreme example is the giant eruption of the massive LBV star  $\eta$  Carinae, which is estimated to have cumulatively lost 2-10  $M_\odot$  between 1840-1860 (Davidson & Humphreys 1997; Smith

2002), representing a mass loss rate  $\sim 0.1 - 0.5 M_{\odot}/\text{yr}$  that is about a factor 10,000 times greater than can be readily explained via the line-driven wind formalism. Instead, the observational association of these LBV's as being near an apparent upper limit in luminosity for observed stars (Humphreys & Davidson 1979, 1984) has led to the general view that the strong mass loss may instead stem from the star approaching or exceeding the so-called “Eddington limit”, at which even the *continuum* force associated with perhaps just electron scattering exceeds the inward force of gravity.

But a key difficulty in understanding how the approach or breach of the Eddington limit might lead to stellar mass loss lies in the fact that both the radiative acceleration and gravity have a similar inverse-square scaling with radius, implying that their ratio  $\Gamma$  (the so-called Eddington parameter) has (in simple 1-D models) a nearly spatially constant value throughout the star. As such, reaching or exceeding the Eddington limit  $\Gamma \geq 1$  would appear to leave the entire star gravitationally unbound, and so does not constitute an appropriate description for steady-state, *surface* wind mass loss from an otherwise stably bound central star.

A promising solution to this difficulty lies in relaxing the usual assumption of strictly one-dimensional (1-D) spherically symmetric stratification, and considering how the lateral structuring – or “porosity” – of a medium could lead to an effective *reduction* in the coupling between the radiation and matter (Shaviv 1998, 2000). In principal, this can provide a way for quasi-stationary wind outflows to be maintained from objects that formally exceed the Eddington limit. A key insight regards the fact that, in a spatially inhomogeneous atmosphere, the radiative transport should selectively avoid regions of enhanced density in favor of relatively low-density, porous channels between them. This stands in contrast to the usual picture of simple 1-D, gray-atmosphere models, wherein the requirements of radiative equilibrium ensure that the radiative flux must be maintained regardless of the medium’s optical thickness. In 2-D or 3-D porous media, even a gray opacity can lead to a flux avoidance of the most optically thick regions, much as in frequency-dependent radiative transfer in a 1-D atmosphere, where the flux avoids spectral lines or bound-free edges that represent spectrally localized regions of non-gray enhancement in opacity. In such a case, the force opacity can be significantly smaller than the Rosseland mean opacity.

In a gray but porous super-Eddington medium, the associated reduction in the coupling of the denser, more optically thick regions of the atmosphere can bring the *effective* Eddington parameter below unity, and thus allow for a stably stratified medium. But as the density decreases outwards and the individual structures become more optically thin, they are again exposed to the full radiation. In a formally super-Eddington medium, the location where the effective Eddington parameter exceeds unity can therefore mark the initiation of the net outward acceleration for a stellar wind (Shaviv 2001b).

In principal, the full solution for a wind outflow in this case requires self-consistent dynamical solution of both the formation of the lateral structure, as well as multi-dimensional transport of the radiation to determine the effective radiative acceleration throughout the

thick to thin regions of the medium. As this represents a quite challenging and computationally intensive effort, it seems appropriate first to seek the development of simpler, perhaps phenomenological approaches that can provide some basic insights into the key properties of wind structure and the likely scalings of the resultant mass loss rates and flow speeds with relevant parameters. Moreover, phenomenological approaches have the advantage that their results can more easily be implemented in more complex systems.

The aim of this paper is to offer such a simplified, heuristic approach, one that takes particular advantage of insights and analogies from the much more well-established theory for line-driven winds. In the following we thus begin (§2) with a general overview of the basic properties and scalings of the standard CAK wind formalism for driving by a power-law ensemble of spectral lines. We next (§3) discuss how the loss of radiative energy, or “photon tiring”, places a fundamental limit on both line- and continuum-driven mass loss, and then (§4) review how a super-Eddington condition in the deeper layers of star can instead lead to convection, pressure inversion, and generally a highly structured medium. To account for the associated porosity reduction in the radiative driving, we next (§5) introduce a simple clump-absorption formalism that, in conjunction with a new “porosity length” *ansatz* (somewhat analogous to the mixing length formalism for convective energy transport) allows the estimation of the porosity-moderated mass loss rate. Drawing on analogies with the CAK model for line-driving, we then (§6) develop a *power-law* porosity formalism and apply this to derive scalings for the mass loss rate and solutions for the wind velocity law. A discussion section (§7) then compares these scalings with previous porosity models, and with inferred observational properties of the giant eruption in  $\eta$  Carinae, including its bipolar form. We conclude (§8) with a general summary and outlook for future work.

## 2. RADIATIVELY DRIVEN MASS-LOSS BY LINE AND/OR CONTINUUM OPACITY

### 2.1. General Equation of Motion

Consider a steady-state stellar wind outflow in which the net acceleration  $v(dv/dr)$  in the radial flow speed  $v(r)$  at radius  $r$  results from a radiative acceleration  $g_{\text{rad}}$  that overcomes the inward gravitational acceleration,  $GM_*/r^2$ ,

$$v \frac{dv}{dr} = -\frac{GM_*}{r^2} + g_{\text{rad}} - \frac{1}{\rho} \frac{dP}{dr}, \quad (1)$$

where the mass density  $\rho$  and the gas pressure  $P = \rho a^2$  are related (by the perfect gas law) through the isothermal sound speed  $a$ . Using the steady-state equation of mass continuity ( $\rho v r^2 = \text{constant}$ ) to eliminate the density  $\rho$ , eqn. (1) takes the form

$$\left[1 - \frac{a^2}{v^2}\right] v \frac{dv}{dr} = -\frac{GM_*}{r^2} + g_{\text{rad}} + \frac{2a^2}{r} - \frac{da^2}{dr}, \quad (2)$$

where the terms containing the isothermal sound speed  $a$  arise from the gas pressure gradient. The square-bracket factor on the left-hand-side (LHS) allows for a smooth mapping of the wind base onto a hydrostatic atmosphere below the sonic point, where  $v < a$ . But in radiatively

driven winds the pressure terms on the right-hand-side (RHS) are generally negligible since, compared to the gravitational acceleration term that must be overcome to drive a wind, these are of order  $w_s \equiv (a/v_{esc})^2 \approx 0.001$ , where  $v_{esc} \equiv \sqrt{2GM_*/R_*}$  is the escape speed from the stellar surface radius  $R_*$ . In the development here, we consequently drop these RHS gas pressure terms, but for now still retain the LHS factor to allow the option of deriving wind solutions that map smoothly onto a hydrostatic atmosphere.

Since the key to a stellar wind is to overcome gravity, it is convenient to define a dimensionless equation of motion that scales all the accelerations by gravity,

$$(1 - w_s/w) w' = -1 + \Gamma_{rad}, \quad (3)$$

where  $\Gamma_{rad} \equiv g_{rad} r^2 / GM_*$ , and the gravitationally scaled inertial acceleration is

$$w' \equiv \frac{r^2 v dv / dr}{GM_*}. \quad (4)$$

In terms of an inverse radius coordinate  $x \equiv 1 - R_*/r$ , note that  $w' = dw/dx$ , where  $w \equiv v^2/v_{esc}^2$  represents the ratio of wind kinetic energy to the gravitational binding  $v_{esc}^2/2 \equiv GM_*/R_*$  from the stellar surface radius  $R_*$ .

For isotropic opacity the dimensional radiative acceleration is set by integration over frequency  $\nu$  of the star's radiative flux  $F_\nu$  weighted by the opacity  $\kappa_\nu$

$$g_{rad} = \int_0^\infty d\nu \kappa_\nu F_\nu / c. \quad (5)$$

In the common, simple case of a continuum dominated by free electron scattering, the opacity  $\kappa_e (= 0.2(1 + X) cm^2/g$  for fully ionized plasmas with hydrogen mass fraction  $X$ , which we take here to have the standard cosmic value  $X \approx 0.7$ ) is strictly gray (frequency independent), allowing it to be pulled out of the frequency integration. This yields an associated acceleration

$$g_e = \kappa_e F / c = \frac{\kappa_e L_*}{4\pi r^2 c}, \quad (6)$$

where  $L_*$  is the star's bolometric luminosity. In the associated gravitationally scaled acceleration, the inverse-radius-squared dependence of the flux cancels with that from gravity, yielding the so-called Eddington parameter

$$\Gamma_e = \frac{\kappa_e L_*}{4\pi GM_* c}, \quad (7)$$

which for 1-D radiative transport in the outer envelope and surface layers is a *spatial constant*, set by the ratio  $L_*/M_*$  of stellar luminosity to mass.

This lack of spatial modulation presents a key difficulty for driving a steady wind mass loss by electron scattering, since a wind requires an outward acceleration that transitions from less than gravity in the interior to above gravity in the outflowing surface layers. As we discuss below (§5 & 6), development of lateral structure can lead to a porosity moderation of continuum driving that allows such a quasi-steady mass loss.

## 2.2. CAK Formalism and Scalings for Line-Driven Stellar Winds

The most well-established formalism for radiative driving in massive stars invokes the operation of *line* opacity

from bound-bound transitions, as first worked out in detail by CAK. As resonant processes, bound transitions have inherently large cross-sections, but only for radiation within a narrow frequency band of width  $\Delta\nu \ll \nu_l$  centered on some line-center resonance frequencies  $\nu_l$ . In the dense layers of a star, the diffusion of radiative energy means that the flux is reduced in proportion to the enhanced opacity, keeping the effective line force small (see eqn. 5). But within the outflowing wind, the Doppler shift of the line-resonance out of the absorption shadow of underlying material exposes the line opacity to a less attenuated flux, and so can lead to a strong radiative force.

Consider for example the case of a single isolated line of resonance frequency  $\nu_l$  within the stellar flux spectrum  $F_\nu$ , with integrated strength  $\kappa_l \Delta\nu / \nu_l \equiv q \kappa_e$  over frequency width  $\Delta\nu$ . For the simple case of radially streaming radiation in a supersonic flow, the use of approximations introduced by Sobolev (1960) gives the ratio of the line acceleration to gravity the scaling

$$\Gamma_q = W_\nu \Gamma_e \frac{1 - e^{-qt_e}}{t_e}, \quad (8)$$

where  $W_\nu = \nu_l F_\nu / F$  is a line flux weight,  $q$  is the dimensionless measure of line opacity, and  $t_e \equiv \rho \kappa_e c / (dv/dr)$  is the radial ‘‘Sobolev optical depth’’ of a line with  $q = 1$ . An important aspect of this form is that it allows evaluation of the radiative acceleration in terms of strictly *local* quantities, namely the density  $\rho$ , velocity gradient  $dv/dr$ , and line strength  $q$ .

A key advance of the CAK analysis was to introduce a formalism for including the cumulative effect of a large number of lines of varying strengths  $q$ , under the simplifying assumptions that these are independent. The central ansatz is that the flux-weighted number distribution of lines is a power law in line-strength

$$q \frac{dN}{dq} = \frac{1}{\Gamma(\alpha)} \left[ \frac{q}{\bar{Q}} \right]^{\alpha-1}, \quad (9)$$

where  $\Gamma(\alpha)$  is the complete Gamma function, and  $\alpha$  is the CAK exponent. Here the line normalization  $\bar{Q}$  is related to the usual CAK  $k$  parameter through  $k = \bar{Q}^{1-\alpha} (v_{th}/c)^\alpha / (1-\alpha)$ ; it offers the advantages of being a dimensionless measure of line-opacity that is independent of the assumed ion thermal speed  $v_{th}$ , with a nearly constant characteristic value of order  $\bar{Q} \sim 10^3$  for a wide range of ionization conditions (Gayley 1995).

Integrating the single-line force (8) over the distribution (9), we obtain for the ratio of the CAK line force to gravity

$$\Gamma_{CAK} = \frac{\bar{Q} \Gamma_e}{(1-\alpha)(\bar{Q} t_e)^\alpha} \equiv C (w')^\alpha. \quad (10)$$

In the latter definition, we have eliminated the density  $\rho$  (within  $t_e$ ) in favor of the mass loss rate  $\dot{M} = 4\pi r^2 \rho v$  for the assumed steady, spherical expansion, with the line-force constant defined by

$$C \equiv \frac{1}{1-\alpha} \left[ \frac{L_*}{\dot{M} c^2} \right]^\alpha [\bar{Q} \Gamma_e]^{1-\alpha}. \quad (11)$$

Note that, for fixed sets of parameters for the star ( $L_*$ ,  $M_*$ ,  $\Gamma_e$ ) and line-opacity ( $\alpha$ ,  $\bar{Q}$ ), this constant scales with the mass loss rate as  $C \propto 1/\dot{M}^\alpha$ .

As already noted, the smallness of the dimensionless sound-speed parameter  $w_s \approx 0.001 \ll 1$  implies that gas pressure plays little role in the dynamics of any radiatively driven stellar wind. Hence to a good approximation, we can obtain accurate solutions by analyzing the much simpler limit of vanishing sound speed  $a \propto \sqrt{w_s} \rightarrow 0$ , for which the line-driven-wind equation of motion reduces to

$$w' + 1 - \Gamma_e = C(w')^\alpha. \quad (12)$$

Since the parameters  $\Gamma_e$  and  $C$  are spatially constant, the solution is independent of radius. For high  $\dot{M}$  and so small  $C$  there are no solutions, while for small  $\dot{M}$  and high  $C$  there are two solutions. The CAK critical solution corresponds to a *maximal* mass loss rate, and requires a *tangential* intersection between line-force and combined inertia plus gravity, for which

$$\alpha C_c w_c'^{\alpha-1} = 1, \quad (13)$$

and thus

$$w_c' = (1 - \Gamma_e) \frac{\alpha}{1 - \alpha}, \quad (14)$$

with

$$C_c = \frac{1}{\alpha^\alpha} \left[ \frac{1 - \Gamma_e}{1 - \alpha} \right]^{1-\alpha}. \quad (15)$$

Using eqn. (11), this then yields the standard CAK scaling for the mass loss rate

$$\dot{M}_{CAK} = \frac{L_*}{c^2} \frac{\alpha}{1 - \alpha} \left[ \frac{\bar{Q}\Gamma_e}{1 - \Gamma_e} \right]^{(1-\alpha)/\alpha}. \quad (16)$$

Moreover, since the scaled equation of motion (12) has no explicit spatial dependence, the scaled critical acceleration  $w_c'$  applies throughout the wind. This can therefore be trivially integrated to yield

$$w(x) = w(1)x \quad (17)$$

where  $w(1) = (1 - \Gamma_e)\alpha/(1 - \alpha)$  is the terminal value of the scaled flow energy. In terms of dimensional quantities, this represents a specific case of the general “beta”-velocity-law,

$$v(r) = v_\infty \left( 1 - \frac{R_*}{r} \right)^\beta, \quad (18)$$

where here  $\beta = 1/2$ , and the wind terminal speed  $v_\infty = v_{esc} \sqrt{\alpha(1 - \Gamma_e)/(1 - \alpha)}$  scales with  $v_{esc} \equiv \sqrt{2GM_*/R_*}$ , the escape speed from the stellar surface radius  $R_*$ .

### 2.3. Extensions of the Basic CAK Theory

Modern implementations of CAK theory have included refinements to account for proper integration of the finite-angle stellar disk (Friend & Abbott 1986; Pauldrach, Puls, & Kudritzki 1986), and ionization state variations with radius (Abbott 1980; Pauldrach 1987; Kudritzki et al. 1989). Together with corrections for a non-zero gas pressure (see appendix of Owocki & ud-Doula 2004), these typically only introduce order-unity corrections to the above theory, and so the scalings derived here still form a good general base to compare with continuum-driven formalism we develop below.

Another important extension regards the role of multi-line scattering, which occurs whenever the velocity separation between optically thick lines obeys  $\Delta v < v_\infty$ . Analyses by Friend & Castor (1982) and Gayley, Owocki, & Cranmer (1995) show, however, that the same CAK scalings still roughly apply as long as the spectral distribution of lines is uniform (i.e., follows Poisson statistics). The total wind momentum then scales as  $\dot{M}v_\infty \approx (v_\infty/\Delta v)L_*/c$ , thus providing a potential line-driven model for the dense winds of WR stars, which are generally inferred to exceed the single scattering limit  $\dot{M}v_\infty = L_*/c$ , sometimes by a factor of 10 or more.

Finally, because of its relevance to our development below of a continuum-driving model, we note in passing another modest conceptual modification to classic CAK theory, namely to account for the fact that, in any discrete distribution of lines, the power-law number approximation should be truncated at a line-strength corresponding the strongest, discrete line. Using an exponential truncation at a line strength  $q_{max} = \bar{Q}$  (at which  $q(dN/dq) \approx 1$ ), the modified, gravity-scaled CAK line force becomes

$$\Gamma_{lines} = \Gamma_{CAK} \left[ (1 + 1/\bar{Q}t_e)^{1-\alpha} - (1/\bar{Q}t_e)^{1-\alpha} \right]. \quad (19)$$

In luminous stars with  $\Gamma_e$  within a factor few of unity, the scaled CAK line force is of order  $\Gamma_{CAK} \approx 1 - \Gamma_e$ , implying that  $\bar{Q}t_e \approx (\bar{Q}\Gamma_e/(1 - \Gamma_e))^{1/\alpha} \gg 1$ , since typically  $\bar{Q} \approx 10^3$ . In such cases, the square bracket correction in eqn. (19) is therefore very nearly unity. For lower luminosity stars, however, this square-bracket corrects the CAK line-force scaling to impose an overall upper limit  $\Gamma_{lines} \leq \bar{Q}\Gamma_e$ . Since a wind requires the driving force to exceed gravity,  $\Gamma_{lines} > 1$ , this shows that normal line-driven mass loss is only possible for stars with  $\Gamma_e > 1/\bar{Q}$ .

### 3. “PHOTON TIRING” AS A FUNDAMENTAL LIMIT TO MASS LOSS

#### 3.1. Line-Driven Winds near the Eddington Limit

As a star approaches the classical Eddington limit  $\Gamma_e \rightarrow 1$ , the standard CAK scalings predict the mass loss rate to diverge as  $\dot{M} \propto 1/(1 - \Gamma_e)^{(1-\alpha)/\alpha}$ , but with a vanishing terminal flow speed  $v_\infty \propto \sqrt{1 - \Gamma_e}$ . The former might appear to provide an explanation for the large mass losses inferred in LBV’s, but the latter fails to explain the moderately high inferred ejection speeds, e.g. the 500-800 km/s kinematic expansion inferred for the Homunculus nebula of  $\eta$  Carinae (Smith 2002).

Moreover, of course, such a divergence of the mass loss rate is precluded by the finite energy available in the stellar luminosity  $L_*$ , which sets a so-called “photon-tiring” limit for lifting mass out of the gravitational potential from the stellar surface (Owocki & Gayley 1997),

$$\dot{M}_{tir} = \frac{L_*}{v_{esc}^2/2} = \frac{L_*}{GM_*/R_*} = 0.032 \frac{M_\odot}{\text{yr}} L_6 \frac{R_*/M_*}{R_\odot/M_\odot}, \quad (20)$$

where  $L_6 \equiv L_*/10^6 L_\odot$ . Comparison with eqn. (16) shows that photon tiring would limit CAK winds whenever

$$1 - \Gamma_e < \bar{Q}\Gamma_e \left[ \frac{\alpha}{1 - \alpha} \frac{v_{esc}^2}{2c^2} \right]^{\alpha/(1-\alpha)}. \quad (21)$$

For typical parameters  $\bar{Q} \approx 2000$  and  $v_{esc}^2/2c^2 \approx 10^{-5}$ , we find that for  $\alpha = 2/3$  photon tiring does not become

important until the star is *very* close to the Eddington limit,

$$1 - \Gamma_e < 2000 [2 \times 10^{-5}]^2 = 8 \times 10^{-7} ; \quad \alpha = 2/3. \quad (22)$$

However, for just a somewhat smaller CAK power index  $\alpha = 1/2$ , the condition is *much* less stringent,

$$1 - \Gamma_e < 2000 [10^{-5}] = 2 \times 10^{-2} ; \quad \alpha = 1/2. \quad (23)$$

This emphasizes that the CAK mass loss rate is extremely sensitive to the power index  $\alpha$ , particularly near the Eddington limit, where the term within the square bracket in eqn. (16) has a large numerical value, which is then raised to a power that depends on  $\alpha$ .

### 3.2. Photon Tiring in Continuum-Driven Mass Loss

Let us now examine photon tiring for continuum-driven flows, ignoring the effect of line-opacity, and simply considering that the continuum opacity now has a known radial dependence  $\kappa_c(r)$ . Specifically, we assume this opacity *increases outward* until some layer becomes super-Eddington, i.e.,  $\Gamma_c > 1$ , where now  $\Gamma_c(r) \equiv \kappa_c(r)L_*/4\pi GM_*c$  is the generalized continuum Eddington parameter. Defining for convenience the radius  $r = R_*$  to be the radius at which  $\Gamma_c(R_*) = 1$ , let us assume moreover that this represents the sonic point of an initiated steady-wind outflow. The density  $\rho_*$  and sound speed  $a_*$  at this point set the mass loss rate  $\dot{M} = 4\pi R_*^2 \rho_* a_*$ , but otherwise gas pressure terms have negligible effect in the further supersonic acceleration of the outflow.

In terms of the scaled wind energy  $w$  and scaled inverse radius  $x$  defined in §2.1, eqn. (3) again represents the scaled equation of motion, with  $\Gamma_{rad} = \Gamma_c(x)$ . Note, however, that in this form in which  $\Gamma_c(x)$  is presumed to be a known spatial function, the mass loss rate itself has scaled out, so that the resulting velocity law would be entirely independent of the amount of mass accelerated.

More realistically, as noted above, a given radiative luminosity can only accelerate a limited mass loss rate before the energy expended in accelerating the outflow against gravity would necessarily come at the expense of a notable reduction in the radiative energy flux itself. To take account of this photon tiring, we must reduce the radiative luminosity according to the gained kinetic and potential energy of the flow,

$$L(r) = L_* - \dot{M} \left[ \frac{v^2}{2} + \frac{GM_*}{R_*} - \frac{GM_*}{r} \right], \quad (24)$$

which implies for the tiring-corrected Eddington parameter that

$$\Gamma_{rad}(x) = \Gamma_c(x) [1 - m(w + x)], \quad (25)$$

where the gravitational “tiring number”,

$$m \equiv \frac{\dot{M}}{\dot{M}_{tir}} = \frac{\dot{M}GM_*}{L_*R_*} \approx 0.012 \frac{\dot{M}_{-4}V_{1000}^2}{L_6}, \quad (26)$$

characterizes the fraction of radiative energy lost in lifting the wind out of the stellar gravitational potential from  $R_*$ . The last expression allows easy evaluation of the likely importance of photon tiring for characteristic scalings, where  $\dot{M}_{-4} \equiv \dot{M}/10^{-4} M_\odot/\text{yr}$ ,  $L_6 \equiv L_*/10^6 L_\odot$ , and  $V_{1000} \equiv v_{esc}/1000 \text{ km/s} \approx 0.62 (M_*/R_*)/(M_\odot/R_\odot)$ .

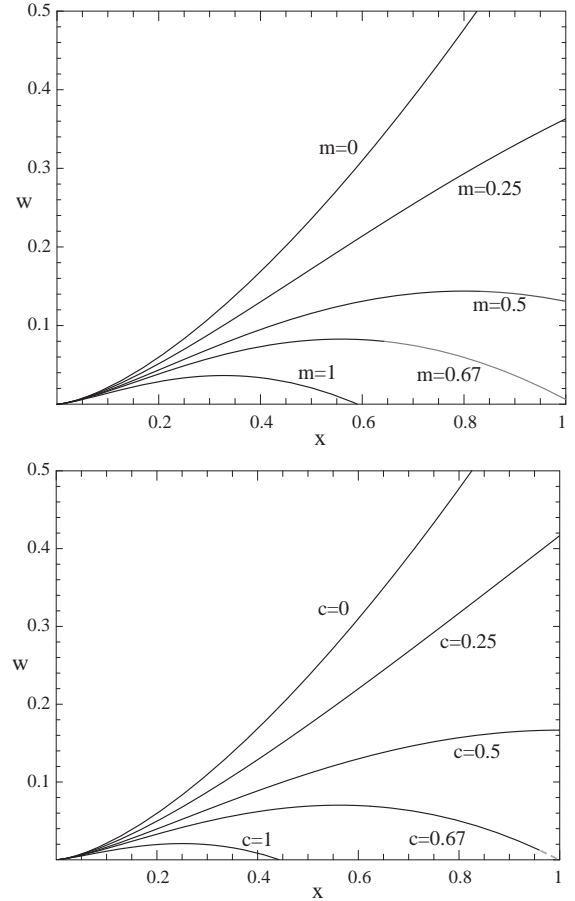


FIG. 1.— a. Wind energy  $w$  vs. scaled inverse radius  $x (\equiv 1 - R_*/r)$ , plotted for Eddington parameter  $\Gamma_c(x) = 1 + \sqrt{x}$  with various photon tiring numbers  $m$ . b. Same as (a), except for weak tiring limit  $m \ll 1$ , and for various constants  $c$  in the Eddington parameter scaling  $\Gamma_c(x) = 1 + \sqrt{x} - 2cx$ .

Applying the tiring-corrected Eddington parameter eqn. (25) into the dimensionless equation of motion (3), we find

$$\left(1 - \frac{w_s}{w}\right) \frac{dw}{dx} = -1 + \Gamma_c(x)[1 - m(w + x)], \quad (27)$$

where for typical hot-star atmospheres the sonic-point boundary value is very small,  $w(0) = w_s = w_* \equiv a_*^2 R_*/2GM_* < 10^{-3}$ . Through most of the wind acceleration, i.e., except near the sonic point itself, the sound-speed term with  $w_*$  can thus be neglected. In the idealized limit  $w_* \rightarrow 0$ , we can use integrating factors to obtain an explicit solution to  $w(x)$  in terms of the integral quantity  $\bar{\Gamma}_c(x) \equiv \int_0^x dx' \Gamma_c(x')$ ,

$$w(x) = -x + \frac{1}{m} \left[ 1 - e^{-m\bar{\Gamma}_c(x)} \right]. \quad (28)$$

As a simple example, consider the case<sup>1</sup> with  $\Gamma_c(x) = 1 + \sqrt{x}$ , for which  $\bar{\Gamma}_c = x + 2x^{3/2}/3$ . Fig. 1a plots solutions  $w(x)$  vs.  $x$  from eqn. (28) with various  $m$ . For low  $m$ , the flow reaches a finite speed at large radii ( $x = 1$ ), but for high  $m$ , it curves back, stopping at some finite *stagnation*

<sup>1</sup> The choice of these functions is arbitrary, to illustrate the photon-tiring effect within a simple model. More physically motivated models based on a medium's porosity are presented in § 6.4.

point  $x_s$ , where  $w(x_s) \equiv 0$ . The latter solutions represent flows for which the mass loss rate is too high for the given stellar luminosity to be able to lift the material to full escape at large radii. By considering the critical case  $w(x=1) = 0$ , we can define a maximum mass loss rate from  $m_{max}$ , given from eqn. (9) by the transcendental relation,

$$m_{max} = 1 - e^{-m_{max}\bar{\Gamma}_c(1)} \approx 1 - e^{2-2\bar{\Gamma}_c(1)}, \quad (29)$$

where the last expression provides a simple explicit approximation<sup>2</sup> for any realistic  $\bar{\Gamma}_c(1) > 1$ . Note that regardless of how large  $\bar{\Gamma}_c(1)$  becomes, it is always true that  $m_{max} < 1$ , simply reflecting the fact that the mass loss is always limited by the rate at which the radiative luminosity can lift material out of the gravitational potential from  $R_*$ . For a given photon tiring number  $m < 1$ , the minimum integrated Eddington parameter required to ensure full escape from the potential is

$$\bar{\Gamma}_c(1) = \frac{-\ln(1-m)}{m}. \quad (30)$$

Even without photon tiring, a similar stagnation can occur from an outward reduction in the radiative driving. In the limit of negligible tiring  $m \ll 1$ , the flow solution (28) simplifies to

$$w(x) \approx \bar{\Gamma}_c(x) - x. \quad (31)$$

For a limited super-Eddington domain, the critical case of marginal escape with zero terminal velocity,  $w(1) = 0$ , is now set in general by the condition  $\bar{\Gamma}_c(1) = 1$ . For example, consider the specific case of a nonmonotonic  $\bar{\Gamma}_c(x) = 1 + \sqrt{x} - 2cx$ , for which then  $\bar{\Gamma}_c(x) = x + 2x^{3/2}/3 - cx^2$ . Fig. 1b plots results for various  $c$ . For all  $\bar{\Gamma}_c(1) < 1$  (i.e.,  $c > 2/3$ ), the material stagnates at the radius where  $\bar{\Gamma}_c(x_s) = x_s = 4/9c^2$ , and so cannot escape the system in a steady-state flow. In a time-dependent model, such material can be expected to accumulate at this stagnation radius, and possibly eventually fall back to the star. This represents another way in which, instead of a steady outflow, a limited super-Eddington region could give rise to an extended envelope with either a mass circulation or a density inversion.

#### 4. STELLAR ENVELOPE CONSEQUENCES OF BREACHING THE EDDINGTON LIMIT

##### 4.1. Convective Instability of Deep Interior

It should be emphasized that locally exceeding the Eddington limit need *not* necessarily lead to initiation of a mass outflow. As first shown by Joss, Salpeter, & Ostriker (1973), in the stellar envelope allowing the Eddington parameter  $\Gamma \rightarrow 1$  generally implies through the Schwarzschild criterion that material becomes *convectively unstable*. Since convection in such deep layers is highly efficient, the radiative luminosity is reduced, thereby lowering the associated radiative Eddington factor away from unity.

This suggests that a radiatively driven outflow should only be initiated *outside* the region where convection is efficient. An upper bound to the convective energy flux is set by

$$F_{conv} \approx v_{conv} l dU/dr \lesssim a H dP/dr \approx a^3 \rho, \quad (32)$$

<sup>2</sup> This has a maximum error of ca. 8%. A somewhat more complex, explicit approximation is  $m_{max} = 1 - \exp[5(1 - \bar{\Gamma}_c(1)^{2/5})]$ , which is accurate to within a half percent.

where  $v_{conv}$ ,  $l$ , and  $U$  are the convective velocity, mixing length, and internal energy density, and  $a$ ,  $H$ ,  $P$ , and  $\rho$  are the sound speed, pressure scale height, pressure, and mass density. Setting this maximum convective flux equal to the total stellar energy flux  $L_*/4\pi r^2$  yields an estimate for the maximum mass loss rate that can be initiated by radiative driving,

$$\dot{M} \leq \frac{L_*}{a^2} \equiv \dot{M}_{max,conv} = \frac{v_{esc}^2}{2a^2} \dot{M}_{tir}, \quad (33)$$

where the last equality emphasizes that, for the usual case of a sound speed much smaller than the local escape speed,  $a \ll v_{esc}$ , such a mass loss would generally be well in excess of the photon-tiring limit set by the energy available to lift the material out of the star's gravitational potential (see eqn. 20). In other words, if a wind were to originate from where convection becomes inefficient, the mass loss would be so large that it would use all the available luminosity to accelerate out of the gravitational potential.

A central conclusion here is accordingly that, while convective transport provides an alternative to a super-Eddington condition in the deep interior, it cannot be the regulation mechanism that would allow for a smooth transition to a steady wind mass loss of the near-surface layers.

##### 4.2. Hydrostatic Pressure Inversion in a Super-Eddington Layer

Even above the inefficient-convection radius, a *limited* super-Eddington domain could, instead of an outflow, merely induce a pressure inversion layer (Maeder 1989), set by integrating the equation of hydrostatic equilibrium (cf. eqn. 1)

$$\frac{d \ln P}{dr} = \frac{\Gamma - 1}{H} \quad (34)$$

where  $H \equiv a^2 r^2 / GM_*$  is the usual gravitational scale height. As an example, for a narrow ( $\Delta r \ll r$ ), isothermal, super-Eddington layer, the pressure would increase by a factor  $\exp[(\Delta r/H)(\bar{\Gamma} - 1)]$ , where  $\bar{\Gamma}$  is the average of  $\Gamma$  over the layer. This exponential pressure increase implies, however, that such inversions are only possible over a limited domain, since eventually the star must match an outer boundary condition of negligible pressure.

Since more realistically the temperature should be expected to decline outward, such a pressure inversion would imply an even stronger outward increase in density. If the super-Eddington condition persists, then perhaps another switch to convective transport could again reduce the radiative flux, and bring the Eddington parameter back below unity. But again this should become inefficient at a layer that cannot maintain an outflow against photon tiring. This implies that any such outflow initiated from the region that convection becomes inefficient would necessarily stagnate at some finite radius. One can imagine that the subsequent infall of material would likely form a complex spatial pattern, consisting of a mixture of both downdrafts and upflows, perhaps even resembling the 3-D cells of thermally driven convection. Overall, we thus see that a star that exceeds the Eddington limit is likely to develop a complex spatial structure, whether due to local instability to convection, or to global instability of flow stagnation. Irrespectively, an inversion or efficient convection cannot

offer a solution giving a photospheric luminosity which is super-Eddington.

#### 4.3. Lateral Instability of Thomson Atmosphere

Dating back to work by Spiegel (1976, 1977) there have been speculations that an atmosphere supported by radiation pressure would likely exhibit instabilities not unlike Rayleigh-Taylor, associated with the support of a heavy fluid by a lighter one, leading to formation of “photon bubbles”. Recent quantitative stability analyses by Spiegel & Tao (1999) and by Shaviv (2001a) do lead to the conclusion that even a simple case of a pure “Thomson atmosphere” – i.e., supported by Thomson scattering of radiation by free electron – would be subject to intrinsic instabilities for development of lateral inhomogeneities. The analysis by Shaviv (2001a) suggests in particular that these instabilities share many similar properties to the excitation of strange mode pulsations (e.g., Glatzel 1994; Papaloizou et al. 1997). For example, they are favored when radiation pressure dominates over gas pressure. Both arise when the temperature perturbation term in the effective equation of state for the gas becomes non-local. In strange mode instabilities, the term arises because the temperature in the diffusion limit depends on the radial gradient of the opacity perturbations. In the lateral instability, the term depends on the lateral radiative flux which arises from non-radial structure on a scale of the vertical scale height.

Note that when conditions of a pure Thomson atmosphere are alleviated, even more instabilities arise. There are of course the aforementioned strange mode instabilities, which require a non-Thomson opacity. If magnetic fields are introduced, even more instabilities can play a role (Arons 1992; Gammie 1998; Begelman 2002; Blaes & Socrates 2003). We stress however that the physical origin of the instabilities is not important to our discussion here. The essential point is merely that as atmospheres approach the Eddington limit, non-radial instabilities do exist to make the atmospheres inhomogeneous, while the typical length scale expected is that of the vertical scale height.

#### 5. SUPER-EDDINGTON OUTFLOW MODERATED BY POROUS OPACITY

Shaviv (2000, 2001b) has applied these notions of a laterally inhomogeneous radiatively supported atmosphere to suggest a new paradigm for how quasi-stationary wind outflows could be maintained from objects that formally exceed the Eddington limit. A key point regards the fact that, in a spatially inhomogeneous atmosphere, the radiative transport will selectively avoid regions of enhanced density in favor of relatively low-density, “porous” channels between them. This stands in contrast to the usual picture of simple 1-D, gray-atmosphere models, wherein the requirements radiative equilibrium ensure that the radiative flux must be maintained independent of the medium’s optical thickness. In 2-D or 3-D porous media, even a gray opacity should lead to a flux avoidance of the most optically thick regions, much as in frequency-dependent radiative transfer in 1-D atmosphere, wherein the flux avoids spectral lines or bound-free edges that represent localized spectral regions of non-gray enhancement in opacity. The associated reduction in the effective opacity might therefore provide

a mechanism for the transition from an effectively sub-Eddington to super-Eddington condition, and perhaps thereby allow an appropriate regulation for steady wind mass loss of the outer layers.

##### 5.1. The Porosity Length and Effective Opacity of a Clumped Medium

The radiative transport in such a complex, 3-D medium is likely to be extremely complicated, but to model the basic elements of this porosity effect, we can consider a simplified picture of a medium consisting of an ensemble of localized clumps or blobs.<sup>3</sup> Assuming for now that the blobs all have the same characteristic length  $l$  and mass  $m_b$ , the characteristic blob density is  $\rho_b \approx m_b/l^3$ , implying in a medium with opacity  $\kappa$  a characteristic blob optical depth  $\tau_b \approx \kappa \rho_b l$ . If the blobs are optically thick,  $\tau_b \gg 1$ , then their effective cross section to impinging radiation is just  $\sigma_{\text{eff}} \approx l^2$ . But more generally, since for arbitrary optical thickness the fraction of impinging radiation attenuated by each blob should scale as  $1 - \exp(-\tau_b)$ , this effective cross section can be written as  $\sigma_{\text{eff}} \approx l^2[1 - \exp(-\tau_b)]$ . From this, we can accordingly define an *effective opacity* of the blobs as

$$\kappa_{\text{eff}} \equiv \frac{\sigma_{\text{eff}}}{m_b} \approx \frac{l^2}{m_b} [1 - \exp(-\tau_b)] \approx \kappa \frac{1 - \exp(-\tau_b)}{\tau_b}. \quad (35)$$

In the limit that the blobs are optically thin,  $\tau_b \ll 1$ , this effective opacity recovers the microscopic value,  $\kappa_{\text{eff}} \approx \kappa(1 - \tau_b/2) \rightarrow \kappa$ . However for optically thick blobs,  $\tau_b \gg 1$ , the opacity is effectively *reduced by a factor*  $1/\tau_b$ , i.e.  $\kappa_{\text{eff}} \rightarrow \kappa/\tau_b \approx l^2/m_b$ .

Let us thus consider a medium that consists entirely of an ensemble of such blobs, with a characteristic separation scale  $L \gg l$ . Then the mean density of the medium is given by  $\rho \approx m_b/L^3 = (l/L)^3 \rho_b$ , and the blob optical thickness can be written as the ratio

$$\tau_b = \frac{\rho}{\rho_c} \quad (36)$$

where the critical medium density at which the blobs have unit optical depth is given by

$$\rho_c \approx \frac{l^2}{\kappa L^3} \equiv \frac{1}{\kappa h}, \quad (37)$$

with the latter equality defining a characteristic “porosity length”  $h \equiv L^3/l^2$ .

As developed further below, this porosity length turns out to be a key parameter for determining the nature and consequences of the porosity in a structured medium. The above shows already that it can have a variety of interpretations:

- As defined here, it is the ratio of the volume per blob to the projected surface area of the blob,  $h = L^3/l^2$ .
- Equivalently, it is the blob size divided by its volume filling factor,  $h = l/(l/L)^3$ .

<sup>3</sup> For comparison, Shaviv (2001b) considered two limiting cases, of either blobs in the optically thin limit or thick but vertically elongated, and a third case of a two phase Markovian mixture. Our analysis here generalizes the first two cases, but is rather different than the statistical description in the third case. Nonetheless, the comparison with the third case reaffirms that the mass loss scaling does not depend on the exact assumed geometry.

- As noted above, the inverse of the porosity length times the opacity defines a critical mean density at which the blobs become optically thick,  $\rho_c \equiv 1/(h\kappa)$ .
- For mean densities above this critical density  $\rho \gg \rho_c$ , it represents the photon *mean-free-path* of the porous medium,  $h = 1/(\kappa_{\text{eff}} \rho) = 1/(\kappa \rho_c)$ , which consequently becomes *independent* of this mean density.

## 5.2. Mass Loss Rate for Model with a Single Porosity Length

Let us now apply this simple picture of a porous medium to model the porosity-moderated mass loss of a super-Eddington atmosphere. The generic mass loss rate can be written as

$$\begin{aligned} \dot{M} &= 4\pi R_*^2 \rho_* a_* \\ &= 4\pi R_*^2 \rho_* a_* \left[ \frac{1}{\rho_c \kappa h} \right] \left[ \frac{HGM_*}{R_*^2 a_*^2} \right] \left[ \frac{\kappa L_*}{\Gamma 4\pi GM_* c} \right] \\ &= \left( \frac{\rho_*}{\rho_c} \right) \left( \frac{H}{h} \right) \left( \frac{1}{\Gamma} \right) \frac{L_*}{a_* c}, \end{aligned} \quad (38)$$

where the basic definition in the first line is multiplied in the second line by a series of unity factors (in square brackets), which are defined in terms of the porosity length  $h$ , the critical density  $\rho_c (= 1/\kappa h)$ , the gravitational scale height  $H (= a_* R_*^2 / GM_*)$ , and the Eddington parameter  $\Gamma (= \kappa L_* / 4\pi GM_* c)$ . After several cancellations, the result in the third line yields three *dimensionless* scale factors (in parenthesis) that multiply the *dimensional* scaling set by the luminosity divided by the product of the speed of light times sound speed. For future reference, we refer to this last factor as the “basal” mass loss rate, with notation

$$\dot{M}_* \equiv \frac{L_*}{a_* c}. \quad (39)$$

So far this is just a simple recasting of the generic mass loss scaling, but it now allows us to apply properties of a specific porosity model to derive associated physical scalings of mass loss from a porosity-moderated, super-Eddington medium.

Let us then first define a scaling for the porosity length  $h$ . For this, consider arguments analogous to those traditionally given for representing convective energy transport in terms of a characteristic “mixing length”, which is generally assumed to scale in proportion to the gravitational scale height  $H$ . Specifically, let us make an analogous *ansatz* that the porosity length should likewise scale with this pressure scale height. We thereby define a dimensionless “porosity-length parameter”,

$$\eta \equiv \frac{h}{H}, \quad (40)$$

which is analogous to the mixing-length parameter,  $\alpha = l_{\text{mix}}/H$ , traditionally assumed for treating convective energy transport.

Note that this scaling relates the porosity length to the pure gas pressure scale height, ignoring any modification due to radiation pressure. A basic justification for this lies in the expectation that the effective Eddington parameter will be substantially reduced in the

porous medium, so that in the final self-consistent state the medium again becomes stratified on a scale proportional to  $H$ . More generally, any effect of radiation pressure in setting this equilibrium can be accounted for by taking this porosity-length parameter to be a function of the Eddington parameter,  $\eta[\Gamma]$ . However, for simplicity, we typically take  $\eta$  to be a fixed independent parameter in the analysis here.

Let us next derive the scaling for the sonic density ratio,  $\rho_*/\rho_c$ . Given a value of the Eddington parameter  $\Gamma > 1$  defined from a microscopic continuum opacity  $\kappa$ , the reduced, effective Eddington parameter for material with arbitrary density  $\rho$  is simply given from application of eqns. (35) and (36),

$$\Gamma_{\text{eff}} = \frac{\kappa_{\text{eff}}}{\kappa} \Gamma \approx \frac{\rho_c}{\rho} \Gamma \left( 1 - e^{-\rho/\rho_c} \right). \quad (41)$$

The reduction at large densities now allows a base hydrostatic region where  $\Gamma_{\text{eff}} < 1$ . The transonic wind is then initiated at the point where  $\Gamma_{\text{eff}} = 1$ , which when applied to eqn. (41) defines an implicit relation for the sonic point density  $\rho_*$ . An *explicit* solution is given by

$$\frac{\rho_*}{\rho_c} = \Gamma + W_0[-\Gamma \exp(-\Gamma)] \approx \Gamma - 1/\Gamma \quad (42)$$

where  $W_0$  represents the principal branch of the *Product-Log* (a.k.a. Lambert) function<sup>4</sup> (Jeffrey, Hare, & Corliss 1996), and the latter, much simpler, approximate form is valid within 6% of the exact solution for all the  $\Gamma > 1$  that are of interest.

Application of the approximate form from (42) into (38) yields the mass loss scaling,

$$\dot{M}_{\text{por}} \approx \left( 1 - \frac{1}{\Gamma^2} \right) \frac{L_*}{\eta a_* c} \quad (43)$$

$$= \left( \frac{\Gamma + 1}{\eta \Gamma} \right) \frac{L_* - L_{\text{Edd}}}{a_* c} \quad (44)$$

$$= \mathcal{W}[\Gamma] \frac{L_* - L_{\text{Edd}}}{a_* c}. \quad (45)$$

The second equality recasts this scaling in terms of a difference of the luminosity from the Eddington luminosity,  $L_{\text{Edd}} \equiv 4\pi GM_* c / \kappa$ . This is quite similar to the scaling derived by Shaviv (2001b), with the final equality introducing his “wind function” (cf. his eqn. 30). In the present formalism this is seen to have the approximate scaling  $\mathcal{W}(\Gamma) \approx (\Gamma + 1)/\Gamma\eta$ , which hence varies from  $\mathcal{W} \approx 2/\eta$  for the marginally super-Eddington case  $\Gamma - 1 \ll 1$  to  $\mathcal{W} \approx 1/\eta$  for the strong super-Eddington limit  $\Gamma \gg 1$ .

In terms of the luminosity-proportional form (43), the dimensional values of the mass loss rate for this single-porosity-length model scale with the basal rate defined in eqn. (39)

$$\begin{aligned} \frac{\eta \dot{M}_{\text{por}}}{1 - 1/\Gamma^2} &\approx \dot{M}_* \equiv \frac{L_*}{a_* c} \\ &= 0.001 \frac{M_\odot}{\text{yr}} \frac{L_6}{a_{20}}, \end{aligned} \quad (46)$$

where  $a_{20} \equiv a_*/20$  km/s and  $L_6 \equiv L_*/10^6 L_\odot$ . Dividing this basal mass loss rate by the tiring-limited value in

<sup>4</sup> <http://mathworld.wolfram.com/LambertW-Function.html>

eqn. (20) gives for the associated “tiring number”

$$m_* \equiv \frac{\dot{M}_*}{\dot{M}_{tir}} = \frac{v_{esc}^2}{2a_*c} = \frac{0.032}{a_{20}} \frac{M_*/R_*}{M_\odot/R_\odot}. \quad (47)$$

We thus see that, under the canonical assumption that  $\eta \approx 1$  (i.e.,  $h \approx H$ ), this single-porosity-length model yields a maximum mass loss rate that is a few percent of the photon tiring limit.

### 5.3. Two-Component Model of Clumps in a Smooth Background Medium

As a next step in developing this phenomenological model for porosity, consider the more realistic case in which these localized blobs are embedded within a smooth, unclumped component. Let us again assume the clumped component consists of many individual blobs with mass  $m_b$  confined to a small size  $l \ll L$  compared to the interblob spacing  $L$ , giving them a density  $\rho_b = m_b/l^3$  that is much larger than the interblob density  $\rho_i = m_i/L^3$ . The density averaged over blob and interblob medium is

$$\bar{\rho} = \frac{m}{L^3} = \rho_i + \rho_b(l/L)^3, \quad (48)$$

where the total mass  $m \equiv m_i + m_b$ .

Again taking the medium to have a fixed microscopic opacity  $\kappa$ , the individual blobs thus now have an optical thickness

$$\tau_b = \kappa \rho_b l = \kappa m_b / l^2 = \kappa \bar{\rho} f L^3 / l^2 = \kappa \bar{\rho} f h, \quad (49)$$

where  $f \equiv m_b/m$  is the blob mass fraction, and  $h \equiv L^3/l^2$  is again the characteristic porosity length. As long as the blobs are optically thin,  $\tau_b \ll 1$ , both the blobs and the interblob medium have this same effective mass-absorption coefficient, namely  $\kappa$ . But if the blobs become optically thick,  $\tau_b \geq 1$ , then, compared to a uniform medium, the effective opacity of this clumped medium is now reduced by a factor

$$\begin{aligned} k &\equiv \frac{\kappa_{\text{eff}}}{\kappa} \\ &= \frac{\kappa m_i + \kappa_b m_b}{\kappa m} \\ &= 1 - f + f \frac{1 - e^{-\tau_b}}{\tau_b} \\ &\equiv k_{\min} + k_b. \end{aligned} \quad (50)$$

Here  $k_{\min} \equiv 1 - f$  represents a minimum value of this effective opacity ratio associated with the interblob medium, while  $k_b$  represents the reduced opacity of the blob component.

It is again instructive to consider a few limiting cases. First, for optically thin blobs  $\tau_b \ll 1$ , we do indeed recover that there is no effective change

$$k \approx 1 - \frac{f\tau_b}{2} + \mathcal{O}(\tau_b^2) \rightarrow 1; \quad \tau_b \ll 1. \quad (51)$$

In the opposite extreme that the medium consists almost entirely of optically thick blobs, with very little interblob material,  $1 - f \ll 1/\tau_b$ , we again find that effective absorption is reduced by a factor given by the inverse of the individual blob optical thickness,

$$k \rightarrow \frac{1}{\tau_b}; \quad 1/(1 - f) \gg \tau_b \gg 1, \quad (52)$$

which in principal can imply quite a substantial reduction in absorption. In the somewhat intermediate case of optically thick blobs with an interblob medium that has a non-negligible mass fraction  $1 - f \gg 1/\tau_b$ , the absorption is dominated by this interblob material, yielding

$$k \rightarrow k_{\min}; \quad \tau_b \gg 1/(1 - f) > 1. \quad (53)$$

This last case represents an important component of added realism for the model, since it implies that, unlike the pure-clumped case considered above, the porosity reduction does not continue to scale in proportion to the inverse density to arbitrarily small values, but rather saturates to a minimum or “floor”,  $k_{\min} = 1 - f$ . More realistically, instead of identical clumps, it seems likely that the structured component may be better modeled as consisting of a broad *distribution* in clump properties, as is developed in the next section.

The general picture then is that, in such a porous medium, the radiative flux, and thus the radiative acceleration, should be weighted towards the lower-density regions, which, in principle can thus have an even greater (super-Eddington) outward driving. However, a further fundamental assumption in the analysis in this paper is that overall medium can still be described in terms of a *single-fluid* model. One justification lies in the relatively high overall densities in the regions of flow initiation – which thus implies a strong gas collisional coupling to share momentum between lower and higher density components. Moreover, since many of the models for structure formation involve travelling wave solutions, the actual material can even alternate in time between dense and rarefied regions, thus implying a further overall averaging in radiative momentum addition. With this overall assumption of strong effective momentum coupling to maintain a single-fluid medium, we thus leave to future studies the issue of possible dynamical differentiation between regions of lower and higher density.

## 6. SUPER-EDDINGTON WIND MODERATED BY A POWER-LAW POROSITY

### 6.1. A Power-Law-Porosity Ansatz

In considering options for further development of this basic formalism, let us first note here an interesting similarity in how both continuum porosity and line opacity lead to a reduced effectiveness in absorption as a function of the relevant optical thickness parameter, viz.  $\tau_b = \kappa \rho h$  vs.  $\tau_l \equiv q \kappa_e \rho c / (dv/dr)$  (see §2.2). Namely, in both cases, the correction factor takes the form  $(1 - e^{-\tau})/\tau$ ; cf. eqns. (8) and (35).

Now, as noted in §2.2, in the theory of line-driven winds a crucial extension over early, single-line analyses (Lucy & Solomon 1970) was the introduction by CAK of a formalism for treating the cumulative effect of many lines.

Likewise, recognizing the unrealistic nature of the above simple picture of a clumped medium in which all the blobs have identical properties, let us next consider a model in which the structured component consists of an *ensemble* of individual clumps with a *range* of optical depths  $\tau_i$ . Compared to a smooth, unclumped medium, the effective opacity of the clump component should then

be reduced by a factor

$$k_b \equiv \frac{\kappa_{\text{eff}}}{\kappa} = \sum_i f_i \frac{1 - e^{-\tau_i}}{\tau_i} \approx \int_0^\infty d\tau \frac{df}{d\tau} \left( \frac{1 - e^{-\tau}}{\tau} \right), \quad (54)$$

where the latter approximation assumes the summation can be approximated by an integral over a suitably defined clump distribution in optical depth,  $df/d\tau$ .

In direct analogy with the CAK power-law formalism for line-strength, let us specifically make the *ansatz* that this distribution can be described by an exponentially truncated power law (see §§2.2 and 2.3, and eqn. 9),

$$\tau \frac{df}{d\tau} = \frac{1}{\Gamma[\alpha_p]} \left( \frac{\tau}{\tau_o} \right)^{\alpha_p} e^{-\tau/\tau_o}, \quad (55)$$

where  $\tau_o$  now represents the optical depth of the *strongest* clump, and  $\alpha_p > 0$  is the power-index<sup>5</sup>. This assumed distribution obeys the normalization

$$\int_0^\infty d\tau \frac{df}{d\tau} \equiv 1. \quad (56)$$

Applying eqn. (55) in eqn. (54), we find the opacity reduction of the clumped medium to be given by (cf. eqn. 10), for  $\alpha_p \neq 1$ ,

$$\begin{aligned} k_b[\tau_o] &= \frac{(1 + \tau_o)^{1-\alpha_p} - 1}{(1 - \alpha_p)\tau_o} \\ &= \frac{[(1 + 1/\tau_o)^{1-\alpha_p} - (1/\tau_o)^{1-\alpha_p}]}{(1 - \alpha_p)\tau_o^{\alpha_p}}, \end{aligned} \quad (57)$$

or for the special case  $\alpha_p = 1$ ,

$$k_b[\tau_o] = \frac{\ln(1 + \tau_o)}{\tau_o}. \quad (58)$$

For fixed clump characteristics, the optical depth  $\tau_o$  again (cf. eqn. 36) scales with the density  $\rho$ ,

$$\tau_o \equiv \frac{\rho}{\rho_o} \quad (59)$$

where the critical density at which this strongest blob has unit optical depth is (cf. eqn. 37)

$$\rho_o = \frac{1}{\kappa h_o}, \quad (60)$$

with  $h_o$  the associated porosity length. This model of a medium with a power-law porosity is now characterized by two parameters, the power index  $\alpha_p$ , and the porosity length  $h_o$  of the strongest blob.

In the limit that even the strongest clump is optically thin,  $\tau_o \ll 1$ , we recover from eqns. (57) and (58) that there is only a small reduction in opacity,

$$k_b[\tau_o] \approx 1 - \alpha_p \tau_o / 2 ; \quad \tau_o \ll 1. \quad (61)$$

In the opposite limit that the strongest clump is optically thick,  $\tau_o \gg 1$ , the asymptotic scaling depends on

<sup>5</sup> We assume that  $\alpha_p > 0$  because otherwise the contribution from weak structure causes the overall number normalization integral (56) to diverge, unless one introduced a further free parameter to cut off the distribution at some minimum porosity length. The subscript “p” stands for porosity, and is added to distinguish this exponent from the usual CAK line-opacity power-index  $\alpha$ . Finally, note that  $\Gamma[\alpha_p]$  represents here the Gamma function, and not the Eddington parameter.

whether  $\alpha_p$  is larger or smaller than one. For  $\alpha_p < 1$ , the square bracket term in (57) approaches unity in this thick limit, and we obtain for the opacity reduction,

$$k_b[\tau_o] \approx \frac{1}{(1 - \alpha_p)\tau_o^{\alpha_p}} ; \quad \tau_o \gg 1 \text{ \& } \alpha_p < 1. \quad (62)$$

For  $\alpha > 1$ , we find

$$k_b[\tau_o] \approx \frac{1}{(\alpha_p - 1)\tau_o} ; \quad \tau_o \gg 1 \text{ \& } \alpha_p > 1. \quad (63)$$

As seen from eqn. (58), the special case  $\alpha_p = 1$  also scales as  $k_b(\tau_o) \propto 1/\tau_o$  in this optically thick limit, but with a proportionality factor that increases logarithmically with optical depth, i.e.,  $\ln(1 + \tau_o)$ .

We thus see that the effective opacity of the structured component can become arbitrarily small at large densities,  $\rho/\rho_o = \tau_o \gg 1$ . However, any “interclump”, *smooth* component should still contribute a constant opacity, independent of density, so that the overall effective opacity is given by

$$k[\tau_o] = k_{\min} + k_b[\tau_o], \quad (64)$$

which thus has a “floor” or minimum effective opacity,  $k_{\min}$ , set the mass fraction of any smooth, interclump component.

## 6.2. Mass Loss Rate for the Power-Law Porosity Model

Let us now apply this power-law porosity model toward computing the mass loss properties from a super-Eddington surface layer. In analogy with eqn. (38), we first write the generic mass loss rate in a form that is scaled by the porosity-length  $h_o$  and the associated critical density  $\rho_o = 1/\kappa h_o$ ,

$$\dot{M} = \left( \frac{\rho_*}{\rho_o} \right) \left( \frac{H}{h_o} \right) \left( \frac{1}{\Gamma} \right) \frac{L_*}{a_* c}. \quad (65)$$

The sonic density  $\rho_*$  is now found through application of eqn. (57) or (58) to the sonic point condition,

$$\Gamma k[\rho_*/\rho_o] = 1, \quad (66)$$

where now we must also require the mass fraction of interclump medium  $k_{\min} < 1/\Gamma$ , so that eqn. (66) has a solution. In the following analyses, we assume this is always the case, regardless of how large  $\Gamma$  becomes. In effect, we thus henceforth effectively take

$$k[\rho/\rho_o] \approx k_b[\rho/\rho_o] ; \quad \rho \leq \rho_*, \quad (67)$$

which applies from the sonic point outward, i.e., through any resulting wind outflow.

In such a medium in which the unclumped Eddington parameter  $\Gamma$  is sufficiently above unity, this sonic point is located where the density is high enough that the strongest clump is quite optically thick,  $\tau_o \gg 1$ . Under this circumstance, the structured component opacity reduction given by the full form (57) can be reduced to the simple power-law forms (62) and (63), thereby allowing trivial solution of the critical condition (66)

$$\frac{\rho_*}{\rho_o} \approx \left[ \frac{\Gamma}{1 - \alpha_p} \right]^{1/\alpha_p} ; \quad \Gamma \gg 1 \text{ \& } \alpha_p < 1, \quad (68)$$

$$\approx \left[ \frac{\Gamma}{\alpha_p - 1} \right] ; \quad \Gamma \gg 1 \text{ \& } \alpha_p > 1. \quad (69)$$

In the opposite limit for which the Eddington parameter is only marginally above unity, we find through application of eqn. (61) in eqn. (66),

$$\frac{\rho_*}{\rho_o} \approx \frac{2(\Gamma - 1)}{\alpha_p} ; \quad \Gamma - 1 \ll 1. \quad (70)$$

For the special case  $\alpha_p = 1/2$ , a general solution to eqn. (66) is

$$\frac{\rho_*}{\rho_o} = 4\Gamma(\Gamma - 1) ; \quad \alpha_p = 1/2. \quad (71)$$

For the special case  $\alpha_p = 1$ , application of eqn. (58) in (66) also yields a general, explicit solution,

$$\frac{\rho_*}{\rho_o} = -1 - \Gamma W_{-1}[-\exp(-1/\Gamma)/\Gamma] \approx 2\Gamma \log(\Gamma) ; \quad \alpha_p = 1, \quad (72)$$

where  $W_{-1}$  is now the lower branch of the Product-Log (Lambert) function (Jeffrey, Hare, & Corliss 1996), and the latter approximation is roughly applicable for moderate  $\Gamma$ , e.g., remaining within ca. 25% of the correct solution for  $\Gamma \leq 10$ .

Next, let us again introduce a *porosity-length parameter*,  $\eta_o \equiv h_o/H$ , relating now to the *strongest* clump (cf. eqn. 40). Applying this, plus eqns. (68)-(72), into eqn. (65), we find the mass-loss rate for the power-law porosity model has the scalings

$$\dot{M}_{pow} \approx \frac{1}{\Gamma} \left[ \frac{\Gamma}{1 - \alpha_p} \right]^{1/\alpha_p} \frac{L_*}{\eta_o a_* c} ; \quad \Gamma \gg 1 \text{ \& } \alpha_p < 1 \quad (73)$$

$$\approx \frac{1}{\alpha_p - 1} \frac{L_*}{\eta_o a_* c} ; \quad \Gamma \gg 1 \text{ \& } \alpha_p > 1 \quad (74)$$

$$\approx \frac{2(\Gamma - 1)}{\alpha_p} \frac{L_*}{\eta_o a_* c} ; \quad \Gamma - 1 \ll 1 \quad (75)$$

$$\approx 2 \log(\Gamma) \frac{L_*}{\eta_o a_* c} ; \quad \alpha_p = 1 \quad (76)$$

$$= 4(\Gamma - 1) \frac{L_*}{\eta_o a_* c} ; \quad \alpha_p = 1/2. \quad (77)$$

It is of interest to compare these results with those given in eqn. (43) for the single-length porosity model of §5.2. For  $\alpha_p > 1$ , eqns. (74) and (75) show that the scaling is similar to the single-length model in both the strongly ( $\Gamma \gg 1$ ) and weakly ( $\Gamma - 1 \ll 1$ ) super-Eddington limits. As noted above, this stems from the fact that in such  $\alpha_p > 1$  models the opacity reduction is dominated by structure with the largest porosity length.

However, for  $\alpha_p \leq 1$ , comparison of eqn. (73) and (43) shows there can be a substantially larger mass loss in the strongly super-Eddington limit of the power-law model. In the single-length model, the opacity in dense layers is reduced by the inverse of the density, but in the  $\alpha_p < 1$  power-law models the reduction is weaker, scaling as  $1/\rho^{\alpha_p}$ . For a large overall Eddington parameter  $\Gamma \gg 1$ , the sonic-point reduction of the effective Eddington to unity occurs at a deeper, denser layer, implying a larger mass loss rate. The net result is to increase the sensitivity of the mass loss rate to the Eddington parameter  $\Gamma$ . For example, for  $\alpha_p = 1/2$ , the overall scaling is in proportion to  $4(\Gamma - 1)$  instead of  $1 - 1/\Gamma^2$ .

Finally, let us consider this power-law-porosity mass-loss relative to the tiring limit discussed in §3. From the

discussion in §5.2 for the single-porosity length model, eqn. (47) already gives the scaling of the tiring number associated with the *basal* mass loss rate,  $\dot{M}_* = L_*/a_*c$ . In the power-law models, the full tiring number is just increased by the additional dimensionless factors from eqns. (73)-(77). For example, for the analytic case  $\alpha_p = 1/2$ , we find the tiring number scales as

$$\begin{aligned} m_{pow} &\equiv \frac{\dot{M}_{pow}}{\dot{M}_{tir}} \\ &\approx 4(\Gamma - 1) \frac{m_*}{\eta_o} \\ &= 0.13 \frac{\Gamma - 1}{\eta_o a_{20}} \frac{M_*/R_*}{M_\odot/R_\odot} ; \quad \alpha_p = 1/2. \end{aligned} \quad (78)$$

We therefore see that, under the canonical assumption that  $\eta_o \approx 1$  (i.e.,  $h_o \approx H$ ) and  $a_{20} \approx 1$ , a porosity model with power index  $\alpha_p = 1/2$  and a moderately large Eddington parameter can readily approach the tiring limit, e.g.,  $m_{pow} \approx 0.52$  for  $\Gamma = 5$ .

Eqn. (78) suggests that while photon tiring should have marginal influence for only mildly super-Eddington models, i.e.,  $\Gamma \lesssim 2$ , it should limit the effective mass loss in strongly super-Eddington cases, i.e.,  $\Gamma > 3$ . We examine this issue further in conjunction with determination of the associated wind velocity law (§6.4).

### 6.3. Wind Velocity Laws for Power-Law Porosity Models without Tiring

In addition to mass loss rate, the power-law porosity formalism can also be used to model the outward wind acceleration and resulting velocity law. Let us first examine this under the assumption that the mass loss rate is small enough that photon tiring can be neglected. Ignoring as before gas pressure effects, the wind acceleration can now be described by the dimensionless equation of motion,

$$w'(x) = \Gamma k[\tau_o(x)] - 1. \quad (79)$$

As above,  $w'$  is the wind acceleration in units of the local gravitational acceleration, and  $x$  is a spatial coordinate defined by  $x \equiv 1 - R_*/r$ , where  $r$  is the local radius and  $R_*$  is a characteristic wind sonic-point radius at which the RHS crosses zero, i.e.,  $w'(0) = \Gamma k[\tau_o(0)] - 1 = 0$ . Applying the opacity reduction eqn. (57), the equation of motion (79) becomes an ordinary, first-order differential equation that can be integrated using standard numerical techniques. The free parameters in this integration are the power-law index  $\alpha_p$ , the Eddington parameter  $\Gamma$ , and the initial flow energy  $w(0) = w_*$ .

Figure 2 shows results for the ratio of wind terminal speed to escape speed  $v_\infty/v_{esc} (\equiv \sqrt{w[1]})$ , plotted vs. Eddington parameter  $\Gamma$  for various  $\alpha_p$  and  $w_*$ . The terminal speeds are typically of order the escape speed, with the larger values for larger  $\Gamma$ , larger  $\alpha_p$ , and lower  $w_*$ .

We also generally find that the height variation of velocity can be reasonably well fit by a modified “beta” velocity law of the form

$$\begin{aligned} v(r) &= \sqrt{a^2 + (v_\infty^2 - a^2) \left(1 - \frac{R_*}{r}\right)^{2\beta}} \\ &\approx v_\infty \left(1 - \frac{R_*}{r}\right)^\beta, \end{aligned} \quad (80)$$

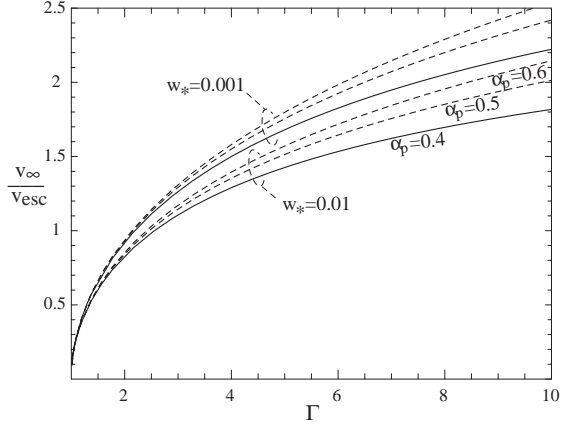


FIG. 2.— Ratio of terminal speed to escape speed,  $v_\infty/v_{esc}$  [ $\equiv \sqrt{w(1)}$ ], plotted as a function of Eddington parameter  $\Gamma$ , for selected values of  $\alpha_p = 0.4, 0.5$ , and  $0.6$  (lower, middle, and upper curves of each triad), and for initial energy  $w_* = 0.01$  (lower triad) and  $w_* = 0.001$  (upper triad). The results can be roughly fit by  $v_\infty/v_{esc} \approx [\log(1/w_*)(\Gamma - 1)/3]^{(1+\alpha_p)/4}$ .

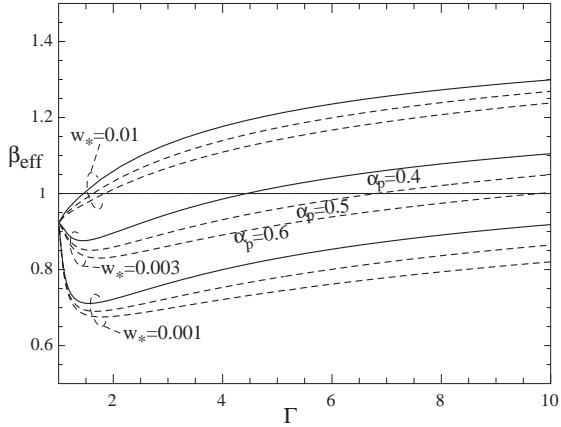


FIG. 3.— Effective velocity law index  $\beta_{\text{eff}}$  ( $\equiv 0.5 \log[(w(1) - w_*)/(w(0.1) - w_*)]$ ) plotted as a function of Eddington parameter  $\Gamma$ , for selected values of  $\alpha_p = 0.4, 0.5$ , and  $0.6$  (lower, middle, and upper curves of each triad), and for initial energy  $w_* = 0.01$  (upper triad),  $w_* = 0.003$  (middle triad), and  $w_* = 0.001$  (lower triad).

with however the velocity power index  $\beta$  dependent on the parameters  $\Gamma$ ,  $\alpha_p$ , and  $w_*$ . To characterize this dependence, we define an effective index

$$\beta_{\text{eff}} \equiv 0.5 \log \left[ \frac{w(1) - w_*}{w(0.1) - w_*} \right], \quad (81)$$

which we find gives a reasonable fit to the numerically integrated velocity variation. Fig. 3 plots  $\beta_{\text{eff}}$  vs.  $\Gamma$  for various  $\alpha_p$  and  $w_*$ . The values are typically within 25% of unity, with larger  $\beta_{\text{eff}}$  occurring for larger  $\Gamma$ , larger  $w_*$ , and smaller  $\alpha_p$ .

By comparison, for line-driven winds typical terminal speeds are 2-3 times the escape speed, with a velocity-law power index  $\beta \approx 0.8 - 1$ . Figs. 2 and 3 show similar results for the power-law porosity model of continuum driving, with however a somewhat wider range that depends on the parameters  $\Gamma$ ,  $\alpha_p$ , and  $w_*$ .

#### 6.4. Photon Tiring and Wind Stagnation for Strongly Super-Eddington Porosity Models

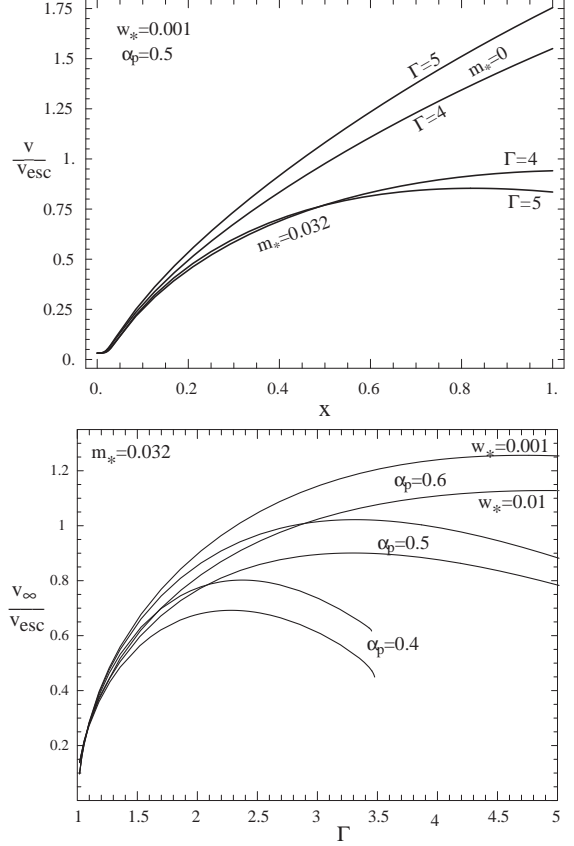


FIG. 4.— a.) Velocity over escape velocity plotted vs. scaled inverse radius  $x$ , for Eddington parameters  $\Gamma=4$  and  $5$ , for models ignoring photon tiring ( $m_* = 0$ ) and with basal tiring parameter  $m_* \equiv v_{esc}^2/2a_*c = 0.032$ . b.) Terminal speed over escape speed, plotted vs. Eddington parameter  $\Gamma$ , for models with basal tiring parameter  $m_* = 0.032$ , with various power-indexes  $\alpha_p$  and initial energies  $w_*$ .

As noted in §6.2, the mass loss rates expected for power-law porosity models with moderately large Eddington parameters ( $\Gamma \gtrsim 3-4$ ) approach the photon tiring limit. Let us now derive velocity solutions for porosity models that take into account photon tiring. From eqns. (27) and (57) the equation of motion now takes the form

$$w'(x) = -1 + k[\tau_o(x)] \Gamma [1 - m(w+x)]. \quad (82)$$

For a given tiring number  $m$ , this can again be integrated numerically from the initial value  $w_*$ , given also the model parameters  $\Gamma$  and  $\alpha_p$ ,

Using eqns. (47) and (65), we can write the tiring number as

$$m = \frac{\rho_* m_*}{\rho_o \eta_o \Gamma} \quad (83)$$

where  $m_* \equiv v_{esc}^2/2a_*c = a_*/2w_*c$ , and  $\rho_*/\rho_o$  is a set by  $\alpha$  and  $\Gamma$  through solution of eqn. (66). For the typical parameters  $\alpha_p = 1/2$  and  $w_* = 0.001$ , figure 4a then plots the velocity over escape velocity,  $v/v_{esc}$ , vs. scaled inverse radius  $x$ , comparing results without tiring ( $m_* = 0$ ) and with the fiducial value of the basal tiring number  $m_* = 0.032$  (eqn. 47). Note that without tiring the velocity is higher for the higher Eddington parameter, but with tiring the velocity is reduced, with the stronger re-

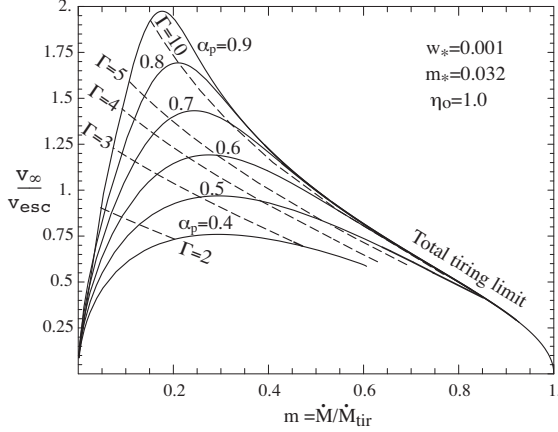


FIG. 5.— Terminal speed over escape speed, plotted vs. photon tiring number  $m \equiv \dot{M}/\dot{M}_{tir}$ , for models with various specific power indices over the range  $\alpha_p = 0.4 - 0.9$  (in increments of 0.1). The dashed curves show contours of the associated Eddington parameter, for the specific values  $\Gamma = 2, 3, 4, 5$ , and  $10$ . The convergence of models along the upper right bound represents the total tiring limit.

duction now making the velocity *lower* for  $\Gamma = 5$  than for  $\Gamma = 4$ .

For this same basal tiring number  $m_* = 0.032$ , Fig. 4b shows the terminal speed over escape speed,  $v_\infty/v_{esc}$ , plotted vs. the Eddington parameter  $\Gamma$ , for selected parameters  $\alpha_p$  and  $w_*$ . Again the tiring reduces the speed, but note that for the lower power index,  $\alpha_p = 0.4$  with moderately large  $\Gamma > 3.5$ , the wind can no longer reach large radii ( $x = 1$ ) with a finite speed.

Fig. 5 plots the ratio of terminal speed to escape speed vs. photon tiring number  $m \equiv \dot{M}/\dot{M}_{tir}$ , for models fixed with the standard parameter set  $\eta_0 = 1$ ,  $m_* = 0.032$ , and  $w_* = 0.001$ , but with various specific power indices over the range  $\alpha_p = 0.4 - 0.9$  (in increments of 0.1). The dashed curves show contours of the associated Eddington parameter, for the specific values  $\Gamma = 2, 3, 4, 5$ , and  $10$ . Note that for lower  $\alpha_p$  and moderately large  $\Gamma$  the tiring becomes substantial. Indeed, the convergence of models along the upper right bound represents the *total* tiring limit, for which the combination of kinetic and potential energy of the wind has exhausted the entire base luminosity  $L_*$ . Hence, models along this limit have little or no remaining luminosity to be observable as radiation.

This illustrates a remarkable property of these power-law porosity models. For small power exponents and moderately large Eddington parameters, they can readily exhaust nearly the entire available luminosity in driving the mass loss.

## 7. DISCUSSION

### 7.1. Comparison with Previous Porosity Analyses

Let us now consider how the above scalings compare with results from previous analyses of porosity-moderated mass loss. Specifically, as noted above (cf. eqn. 45), Shaviv (2001b) has cast the mass loss scaling in terms of a “wind function”  $\mathcal{W}(\Gamma)$  times the deviation of the luminosity from its Eddington limit value,

$$\dot{M} = \mathcal{W}[\Gamma] \frac{L_* - L_{Edd}}{a_* c} = \mathcal{W}[\Gamma] \left( \frac{\Gamma - 1}{\Gamma} \right) \frac{L_*}{a_* c}. \quad (84)$$

As noted in §5.2, for the single-scale porosity model, the wind function  $\mathcal{W}[\Gamma] \approx (\Gamma + 1)/\Gamma\eta$ , which therefore varies from  $\mathcal{W} \approx 2/\eta$  for the marginally super-Eddington case  $\Gamma - 1 \ll 1$  to  $\mathcal{W} \approx 1/\eta$  for the strong super-Eddington limit  $\Gamma \gg 1$ . For comparison, Shaviv (2001b) considered two limiting cases, of either blobs in the optically thin limit or thick but vertically elongated, and a third case of a two phase Markovian mixture. For all cases, he estimated that the wind function would be of order unity, which is indeed our estimate here from the single-scale porosity model.

However, for porosity models with power-indices  $\alpha < 1$ , we find here that there can be a further increase above this basal mass loss of the single-scale model. For example, for the canonical case  $\alpha_p = 1/2$ , comparison of (84) and (77) implies the wind function scaling to be

$$\mathcal{W}[\Gamma] = \frac{4\Gamma}{\eta_0} ; \quad \alpha_p = 1/2. \quad (85)$$

A key new feature of the power-law porosity model is consequently that this wind function increases with the Eddington parameter, and so now can become substantially larger than just the order unity value derived for the single-scale model, and also inferred from the analyses by Shaviv (2001b). Since even the basal mass loss rate (39) for the single-model can be a few percent of the tiring limit (20), the additional increase for moderately large Eddington parameter  $\Gamma > 4 - 5$  can bring the overall mass loss close to this limit.

In addition, of course, the mass loss scaling depends on the scaling of the porosity-length  $h_o$ , and this might also depend on  $\Gamma$ . In particular, we have assumed above that the porosity length scales with the pure-gas-pressure scale height  $H$ ; but in a medium in which there is a residual smooth component that puts a floor  $k_{min}$  in the effective opacity (see §§5.3-6.2), the effective gravitational scale height at large depth is instead given by  $H/(1 - k_{min}\Gamma)$ . Scaling the porosity length scales with this larger stratification height could then reduce the mass loss rate by a factor  $(1 - k_{min}\Gamma)$ , which in the possible case that  $k_{min}\Gamma \lesssim 1$ , could represent a substantial reduction. This general effect was also discussed by Shaviv (2001b).

### 7.2. Comparison to Inferred Mass Loss of Giant Eruptions

Let us next consider the conditions needed for this power-law-porosity model to reach the observationally inferred mass loss rates of giant eruptions of Luminous Blue Variable (LBV) stars like  $\eta$  Carinae. Analyses of the resulting Homunculus nebula (Smith 2002) indicate that during the roughly 20-year outburst from ca. 1840-60,  $\eta$  Carinae lost  $2 - 10 M_\odot$ , representing an average mass loss rate of  $0.1 - 0.5 M_\odot/\text{yr}$ . Moreover, the expansion of the Homunculus nebula is inferred to be in the range  $v_{exp} = 500 - 700 \text{ km/s}$ . If we characterize this expansion velocity as being some order-unity factor of the escape speed from the surface of origin,  $\sqrt{w_\infty} \equiv v_{exp}/v_{esc}$ , then the total luminosity associated with this wind mass loss is

$$\begin{aligned} L_{wind} &= \dot{M} v_{esc}^2 (1 + w_\infty)/2 \\ &= 30 \times 10^6 L_\odot \dot{M}_1 \frac{M_*/R_*}{M_\odot/R_\odot} (1 + w_\infty), \end{aligned} \quad (86)$$

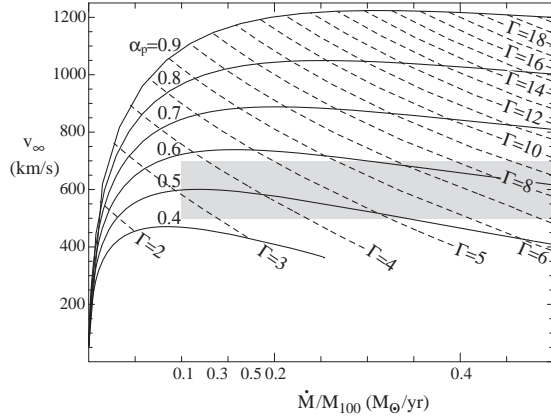


FIG. 6.— Same models as fig. 5, but now for corresponding dimensional values, showing terminal speed vs. mass loss rate (scaled by  $M_{100}$ , the stellar mass in units of  $100 M_{\odot}$ ). The dashed curves again show contours of the Eddington parameter, now for integer values in the range  $\Gamma = 2 - 20$ . Both plot sets assume the same dimensionless parameter combination,  $w_* = 0.001$  and  $m_* = 0.032$ , which together imply dimensional parameters of  $a_* = 20$  km/s for the base sound speed and  $v_{esc} = 620$  km/s ( $= v_{esc,\odot}$ ) for the surface escape speed. The semi-transparent box denotes the observationally inferred parameter range for the 1840-60 giant eruption of  $\eta$  Carinae that gave rise to the Homunculus nebula.

where  $\dot{M}_1 \equiv \dot{M}/(1M_{\odot}/\text{yr})$ . For a solar value of mass to radius,  $v_{esc} \approx 620$  km/s  $\approx v_{exp}$ ; thus, assuming  $w_{\infty} \approx 1$  in this case, we see from eqn. (86) that the observationally inferred range of mass loss for  $\eta$  Carinae requires a total wind luminosity in the range  $L_{wind} \approx 6-30 \times 10^6 L_{\odot}$  (Smith 2002).

Moreover historical observations suggest a radiative luminosity of roughly  $L_{obs} \approx 20 \times 10^6 L_{\odot}$  (Davidson & Humphreys 1997), implying a total luminosity of up to  $50 \times 10^6 L_{\odot}$ !

To facilitate comparisons with these observational values, let us now convert the above dimensionless model results into physical units. The above standard dimensionless parameters  $w_* \equiv (v_{esc}/a_*)^2 = 0.001$  and  $m_* = v_{esc}^2/2a_*c = 0.032$  imply specific dimensional values for the surface escape speed

$$v_{esc} = 2cm_*\sqrt{w_*} \approx 620 \text{ km/s} \approx v_{esc,\odot}, \quad (87)$$

and the surface sound speed

$$a_* = 2cm_*w_* \approx 20 \text{ km/s}. \quad (88)$$

The dimensional value of the terminal speed is thus given by  $v_{\infty} = 620$  km/s  $\sqrt{w[1]}$ . From eqn. (38), the dimensional mass loss is obtained from

$$\dot{M} = 3.9 \times 10^{-3} \frac{M_{\odot}}{\text{yr}} \frac{\rho_*}{\rho_o} \frac{M_{100}}{\eta_o a_{20}}, \quad (89)$$

where  $M_{100} \equiv M_*/100M_{\odot}$  and  $a_{20} \equiv a_*/(20 \text{ km/s})$ .

Fig. 6 plots the terminal speed  $v_{\infty}$  vs. the mass loss rate  $\dot{M}$  for the same models shown in the dimensionless plots of fig. 5, for various power indices  $\alpha_p$ . The dashed curves again show contours of the associated Eddington parameter  $\Gamma$ . The observationally inferred ranges of mass loss and terminal speed are denoted by the shaded box. Assuming a canonical stellar mass  $M_{100} = 1$ , note that even the upper range of mass loss,  $\dot{M}_1 \approx 0.5$ , can be obtained with  $\alpha_p \approx 0.6$  and  $\Gamma \approx 8.5$ .

However, note also from eqn. (86) that the associated wind luminosity for this case is  $L_{wind} \approx 30 \times 10^6 L_{\odot}$ . From the conversion  $\Gamma \approx 0.27L_6/M_{100}$ , this implies an associated “wind Eddington parameter”,  $\Gamma_{wind} \approx 8.1$ , which therefore means that a fraction 8.1/8.5, or about 95%, of the source luminosity is consumed in the wind! This in turn implies that the observable radiative luminosity in such a model would be a mere

$$\begin{aligned} L_{rad,\infty} &\approx (\Gamma - \Gamma_{wind})L_{Edd} \\ &\approx (8.5 - 8.1) 3.7 \times 10^6 L_{\odot} \\ &\approx 1.5 \times 10^6 L_{\odot}, \end{aligned} \quad (90)$$

which is much less than the historically observed value of  $L_{obs} \approx 20 \times 10^6 L_{\odot}$  noted above (Davidson & Humphreys 1997).

Our further analysis indicates that fitting this observed luminosity together with the inferred mass loss and terminal speed requires a *reduction* of the assumed surface escape speed. As shown in fig. 2, without photon tiring the ratio of terminal speed to escape speed increases with increasing Eddington parameter  $\Gamma$ . This is a direct result of the fact that radiative driving scales with  $\Gamma$ , and so as seen from the equation of motion without tiring (eqn. 79) the scaled acceleration likewise increases with  $\Gamma$ . But the mass loss also increases with  $\Gamma$ , and in models with photon tiring, the increased tiring number reduces the driving (see eqn. 82). Thus, as shown in figs. 4 and 5, the terminal speed peaks and then decreases with higher  $\Gamma$ . This makes it possible to obtain both a large mass rate and a modest terminal speed that is equal to the assumed escape speed. But because of the dominant role of tiring, a by-product of such models is that there is little remaining radiative energy to be observed as emergent luminosity.

However, if we assume a lower escape speed, then models with less tiring can produce the observed terminal speed. For example, taking the same stellar mass  $M_{100} = 1$  but an increased stellar radius  $R_{100} = 3$  implies a reduced effective escape speed  $v_{esc} = 360$  km/s, so that the same target expansion speed now requires a speed ratio  $v_{\infty}/v_{esc} = \sqrt{3} \approx 1.73$ , and therefore an energy ratio  $w_{\infty} = 3$ . For the targeted mass loss  $\dot{M}_1 = 0.5$ , we then see from eqn. (86) that the associated wind luminosity is now  $L_{wind} \approx 20 \times 10^6 L_{\odot}$ . Together with the observed luminosity, this requires of total base luminosity of  $L_* \approx 40 \times 10^6 L_{\odot}$ , corresponding to an Eddington parameter  $\Gamma \approx 10.8$ .

By taking this  $L_*$  with  $M_{100} = 1$  and  $R_{100} = 3$ , and keeping the remaining three parameters the same ( $\eta_o = 1$ ,  $\alpha = 0.6$ ,  $a_{20} = 1$ ), we then find that the observable radiative luminosity is now higher than before ( $L_{obs} \approx 13.4 \times 10^6 L_{\odot}$ ), but still below the target value, essentially because of too much tiring from the still-too-high mass loss rate ( $\dot{M}_1 \approx 0.76$ ). To reduce the mass loss, we can increase the porosity parameter  $\eta_o$  and/or the sound speed  $a_{20}$ . Choosing the former, we find that  $\eta_o = 1.56$  gives results within 2% of the targeted values for all three observational parameters.

Of course, given that the model has a total of six adjustable parameters, the significance of being able to fit three observed values should not be exaggerated. Nonetheless, it is encouraging that this power-law porosity model can reproduce such rather extreme mass loss

conditions with quite plausible choices of these parameters. It is particularly interesting that, because of the scalings of mass loss and flow speed with the Eddington parameter, and their interplay with photon tiring, reproducing both the inferred mass loss and radiative luminosity requires that the source star's surface escape speed is somewhat smaller than the inferred expansion speed.

### 7.3. Gravity Darkening and the Shaping of LBV Nebulae

For simplicity, the above formalism has assumed a spherically symmetric mass loss, but in the case of  $\eta$  Carinae, the resulting Homunculus nebula exhibits a distinctly bipolar, prolate form. Detailed analysis (Smith 2002) indicates the nebula has both a higher speed and greater density toward the bipolar symmetry axis, suggesting that the 1840-60 giant outburst was itself intrinsically bipolar. Moreover, there is evidence, from both ground-based interferometric observations (van Boekel et al. 2003) and from HST slit-spectra (Smith et al. 2003), the *present-day* wind of  $\eta$  Carinae is also bipolar about the same symmetry axis as the Homunculus.

One promising scenario, first proposed by Owocki & Gayley (1997) and developed further by Maeder & Meynet (2000), Maeder & Desjacques (2000), and Dwarkadas & Owocki (2002), is that such bipolar mass loss is the natural consequence of radiative driving from a nearly critically rotating star with a substantial equatorial *gravity darkening* (von Zeipel 1924). However, since this basic idea arose from models of relatively low-density, *line-driven* winds (Owocki, Cranmer, & Gayley 1996), the applicability to much denser, continuum-driven models for  $\eta$  Carinae or other LBVs has been uncertain. Eventually, the issue should be examined through 2-D dynamical models that account for the latitudinal mass and radiation transport within the optically thick, bipolar expansion.

But for now, it is worth noting that the underlying scalings for the speed and mass flux have some key similarities in both the basic line-driven-wind theory and the present models for porosity-moderated continuum-driving of a dense, optically thick flow. In particular, comparison of eqns. (16) and (73)-(77) shows that the mass loss rate in both cases scales with the stellar luminosity times a correction factor that is a function of the Eddington parameter, i.e.,  $\dot{M} \propto L_* f[\Gamma]$ . Accordingly, in a rotating star, the local surface mass flux  $\dot{m}_*(\theta)$  at any colatitude  $\theta$  should vary in proportion to the local surface radiation flux  $F_*(\theta)$ , times a function of the local effective Eddington parameter  $\Gamma \equiv F_*/g_{\text{eff}}$ , where  $g_{\text{eff}}$  is the effective, centrifugally reduced surface gravity. But for the standard von Zeipel (1924) gravity darkening scaling that  $F_*(\theta) \propto g_{\text{eff}}(\theta)$ , we see that the Eddington parameter is *latitudinally constant*, implying then that the surface mass flux should scale simply as

$$\dot{m}_*(\theta) \propto F_*(\theta) \propto g_{\text{eff}}(\theta). \quad (91)$$

Since both the radiative flux and effective gravity are maximum at the rotational pole, eqn. (91) shows that the mass flux should be strongest near the poles.

Similar arguments can be made for the latitudinal variation of the flow expansion speed. Again, the detailed re-

sults may depend on latitudinal components of the mass flow, radiation flux, and radiative force, and should be eventually be analyzed through 2-D models. But within the context of simple 1-D scaling relations for both line-driven and porosity models, the outflow speed should follow the approximate scaling,

$$v_\infty(\theta) \propto v_{\text{esc}}(\theta) \propto \sqrt{g_{\text{eff}}(\theta)}. \quad (92)$$

Since the effective gravity is highest toward the poles, we can expect the nebula expansion to be faster near the symmetry axis. Observations do indeed show that  $v(\theta)$  for the polar lobes of the Homunculus nebula is roughly proportional to the simple latitudinal variation of escape speed from a rotating star (Smith 2002).

Overall, the expected faster polar flow speed can explain the generally prolate form of the expanding nebula, while the higher polar mass flux can explain the observationally inferred mass concentration near the polar symmetry axis. Thus, an attractive feature of the porosity-moderated continuum-driven formalism is that it preserves these key 1-D flow scalings from line-driven models, while allowing extension to much larger mass loss rates. However, as noted, more complete 2-D models should be developed to examine how these general scalings might be affected by latitudinal mass and radiation transport.

Finally, while several LBV nebulae show such a bipolar or ellipsoidal form, none except maybe HR Carinae is as severely pinched at the equator as  $\eta$  Carinae. P Cygni – the only other Galactic star observed to have a giant eruption approaching the extremity of that in  $\eta$  Carinae – has a nearly spherical ring nebula (Nota & Clampin 1997). In this context, it should be emphasized that the basic porosity model developed here can accommodate a range of geometric forms, depending on the degree of rotation of the source star.

## 8. CONCLUDING SUMMARY

Let us conclude with an itemized summary of the goals, methods, and results of the analyses in this paper.

1. The overall goal is to develop a radiative-driving formalism for explaining the extremely large mass loss rates and moderately high outflow speeds inferred in giant outbursts of Luminous Blue Variables, most particularly the 1840-60 outburst of  $\eta$  Carinae that resulted in the Homunculus nebula. The general approach combines and builds upon two previous models for radiative driving, namely the well-established CAK line-driving generally applied for more quiescent phases of hot-star wind mass loss, and recent notions of porosity-moderated continuum driving in stars that exceed a generalized Eddington limit (Shaviv 1998, 2001b).
2. As a basis for this synthesis, we first review the CAK line-driven formalism, showing thereby that for reasonable values of the line-opacity normalization, the expected wind momentum (i.e., the product of mass loss rate and flow speed) in such models falls well below what is inferred in LBV giant outbursts. The formal divergence in CAK mass loss rate as a star approaches the Eddington limit is accompanied by a vanishing terminal speed, and

- moreover in practice is limited by the “photon tiring” of the finite luminosity available to lift material from the gravitational potential at the stellar surface.
3. In the deep stellar interior, approaching and exceeding the Eddington limit leads to convective energy transport that lowers the radiative flux and allows a normal hydrostatic stratification with outwardly declining pressure and density. In near-surface layers where the lower density makes convective transport inefficient, a super-Eddington condition again implies that the outward radiative force exceeds gravity. Hydrostatic stratification then requires an outward *inversion* of pressure and density, which however can only be maintained over a limited range, given the inherent outer boundary condition of vanishing pressure and density.
  4. Moreover, any outflow initiated where convection first becomes inefficient would imply a huge mass loss rate, of order  $L_*/a_*^2$ , where  $a_*$  is the sound speed; this exceeds by a large factor the “tiring limit” mass loss,  $\dot{M}_{tir} = 2L_*/v_{esc}^2$ , for which the energy expended to lift material from the surface gravitational potential equals the assumed stellar luminosity. The flow stagnation associated with photon tiring, together with other instabilities, seems likely to impart a complex, time-dependent, 3-D structure to the atmosphere of any star that approaches or exceeds the Eddington limit.
  5. As first noted by Shaviv (1998), the “porosity” of such a structured, super-Eddington medium can lower the effective driving opacity in the deeper, denser layers, allowing a base hydrostatic balance that transitions to a supersonic outflow as the structures become optically thin, and hence are again subject to the full radiative force.
  6. We introduce a simple formalism that characterizes this effect in terms of a “porosity length”  $h \equiv L^3/l^2$ , where  $l$  and  $L$  represent the size and separation of individual clumps or blobs. We show that a simple ansatz (somewhat analogous to the mixing length parameterization of convective transport) – that this porosity length is an order-unity factor  $\eta$  times the gravitational scale height  $H$  – leads to a mass loss rate  $\dot{M}_{por} \approx (1 - 1/\Gamma^2)L_*/\eta a_* c$ , a scaling that is very similar to that derived previously by Shaviv (2001b) for both vertical elongation and Markovian mixture models of atmospheric structure. Though large, such mass loss is still typically only a few percent of the tiring limit.
  7. In analogy with the CAK formalism of driving by a power-law ensemble of lines, we then generalize to a “power-law-porosity” treatment, characterized by a power index  $\alpha_p$  and a porosity-parameter  $\eta_o$  for the most optically thick blob. For  $\alpha_p \gtrsim 1$ , the derived mass loss rates are similar to the single-scale model, but for  $\alpha_p < 1$  they lead to enhancement by factors that scale with the Eddington parameter as  $\Gamma^{-1+1/\alpha_p}$ . For large  $\Gamma$ , small  $\alpha_p$ , and/or small  $\eta_o$ , this can now lead to overall mass loss rates that approach the photon tiring limit.

8. Without tiring, the wind velocity follows a canonical “beta-velocity-law” form, with index  $\beta \approx 1$ , and a terminal speed proportional to the escape speed times a factor that scales roughly with  $(\Gamma - 1)^{(\alpha_p+1)/4}$ . With tiring, the velocity law can become nonmonotonic, with a terminal speed that decreases with increasing mass loss rate. Models with a terminal speed less than or equal to the surface escape speed are strongly tired, and so have a greatly reduced observable radiative luminosity.
9. Given stellar parameters  $L_*$ ,  $M_*$ , and  $R_*$ , plus a base sound speed  $a_*$ , the mass loss properties of the power-law-porosity model depend on the power index  $\alpha_p$  and porosity-length parameter  $\eta_o$ . For quite reasonable values, the model can reproduce the observationally inferred mass loss and speed for the giant eruption of  $\eta$  Carinae, but matching also the historically estimated radiative luminosity during this epoch requires a modest surface escape speed, with ratio of stellar mass to radius perhaps a third of the solar value.
10. Though the magnitude of mass loss greatly exceeds what’s feasible with line-driving, the porosity model retains the key scalings with gravity and radiative flux that would give a rapidly rotating, gravity-darkened source star an enhanced polar mass loss and flow speed, as is inferred from the bipolar form of the Homunculus nebula in  $\eta$  Carinae.

Overall, the extended porosity formalism developed here provides a promising basis for self-consistent dynamical modeling of even the most extreme mass loss outbursts of Luminous Blue Variables, namely those that, like the giant eruption of  $\eta$  Carinae, approach the photon tiring limit. But of course much further work will be needed to substantiate and quantify the basic “porosity-length” phenomenology proposed here. Much in the same way that modern-day multi-dimensional simulations of stellar convection have been used to test classical mixing length phenomenology, future work should focus on developing 2-D or 3-D radiation hydrodynamical simulations of the nonlinear evolution of atmospheric structure in stars near and above the Eddington limit. A particular challenge will be to develop fast techniques for treating the multi-dimensional, nonlocal radiation transport in such a medium. Of course, until such more fundamental calculations are carried out, it is difficult to appraise the overall applicability of our porosity-length approach. But in any case the basic phenomenology helps provide a motivation and conceptual framework for carrying out and interpreting such more fundamental and challenging radiation hydrodynamical simulations.

*Acknowledgements.* SPO acknowledges support from NSF grant AST-0097983. NJS acknowledges the support from ISF grant 201/02. We thank K. Davidson, R. Townsend and N. Smith for helpful discussions and comments.

## REFERENCES

- Abbott, D. C. 1980, ApJ, 242, 1183  
 Arons, J. 1992, ApJ, 388, 561  
 Asplund, M. 1998, A&A, 330, 641  
 Begelman, M. C. 2002, ApJ, 568, L97  
 Blaes, O. & Socrates, A. 2003, ApJ, 596, 509  
 Castor, J. I., Abbott, D. C., & Klein, R. I. 1975, ApJ, 195, 157 (CAK)  
 Collins, G. W. & Harrington, J. P. 1966, ApJ, 146, 152  
 Davidson, K. & Humphreys, R. M. 1997, ARA&A, 35, 1  
 Dwarkadas, V. & Owocki, S. P. 2002, ApJ, 581, 1337  
 Friend, D. B. & Abbott, D. C. 1986, ApJ, 311, 701  
 Friend, D. B. & Castor, J. I. 1982, ApJ, 261, 293  
 Gammie, C. F. 1998, MNRAS, 297, 929  
 Gayley, K. G. 1995, ApJ, 454, 410  
 Gayley, K. G., Owocki, S. P., and Cranmer, S. R. 1995, ApJ, 442, 296  
 Glatzel, W. 1994, MNRAS, 271, 66  
 Humphreys, R. M. & Davidson, K. 1979, ApJ, 232, 409  
 Humphreys, R. M. & Davidson, K. 1984, Science, 223, 243  
 Jeffrey, D. J., Hare, D. E. G., Corliss, R. M. 1996, *Math Sci.*, 21, 1  
 Joss, P. C., Salpeter, E. E., & Ostriker, J. P. 1973, ApJ, 181, 429  
 Kudritzki, R. P., Pauldrach, A. W., Puls, J., & Abbott, D. C. 1989, A&A, 219, 205  
 Lucy, L. B. & Solomon, P. M. 1970, ApJ, 159, 879  
 Maeder, A. 1989, in *Physics of Luminous Blue Variables*, IAU Colloquium #113, K. Davidson, A. Moffat, and H. Lamers, eds., Kluwer, Dordrecht, p. 15  
 Maeder, A. & Desjacques, V. 2002, A&A, 372, L9  
 Maeder, A. & Meynet, G. 2002, A&A, 361, 159  
 Nota, A. & Clampin, M. 1997, ASP Conf. Ser. 120, *Luminous Blue Variables: Massive Stars in Transition*, A. Nota & H. Lamers, eds., p. 303  
 Owocki, S. P., Cranmer, S. R., & Gayley, K. G. 1996 ApJ, 472, L115  
 Owocki, S. P. & Gayley, K. G. 1997, ASP Conf. Ser. 120, *Luminous Blue Variables: Massive Stars in Transition*, A. Nota & H. Lamers, eds., p. 121  
 Owocki, S. P. & ud-Doula, A. 2004, ApJ, 600, 1004  
 Papaloizou, J. C. B., Alberts, F., Pringle, J. E., & Savonije, G. J. 1997, MNRAS, 284, 821  
 Pauldrach, A. 1987, A&A, 183, 295  
 Pauldrach, A., Puls, J., & Kudritzki, R. P. 1986, A&A, 164, 86  
 Shaviv, N. J. 1998, ApJ, 494, L193  
 Shaviv, N. J. 2000, ApJ, 532, L137  
 Shaviv, N. J. 2001, ApJ, 549, 1093  
 Shaviv, N. J. 2001, MNRAS, 326, 126  
 Smith, N. 2002, MNRAS, 337, 1252  
 Smith, N., Gehrz, R. D., Hinz, P. M., Hoffmann, W. F., Hora, J. L., Mamajek, E. E., Meyer, M. R. 2003a, AJ, 125, 1458  
 Smith, N., Davidson, K., Gull, T. R., Ishibashi, K., Hillier, D. J. 2003b, ApJ, 586, 432  
 Spiegel, E. A. 1977, IAU Colloq. 38: Problems of Stellar Convection, 267  
 Spiegel, E. A. 1976, Physique des Mouvements dans les Atmospheres, 19  
 Spiegel, E. A. & Tao, L. 1999, Phys. Rep., 311, 163  
 van Boekel, R., Kervella, P., Schiller, M., Herbst, T., Brandner, W., de Koter, A., Waters, L., Hillier, D. J., Paresce, F., Lenzen, R., Lagrange, A.-M. 2003, A&A, 410, L37  
 von Zeipel, H. 1924, MNRAS, 84, 665